

Second species orbits of negative action and contact forms in the circular restricted three-body problem

Robert Nicholls

August 13, 2021

Abstract

We show in this work that the restricted three-body problem is in general not of contact type and zero is the energy value where the contact property breaks down. More explicitly, sequences of generating orbits with increasingly negative action and energies between $-\sqrt{2}$ and zero are constructed. Using results from [BM00], it is shown that these generating orbits extend to periodic solutions of the restricted three-body problem for small mass ratios and the action remains within a small neighbourhood. These orbits obstruct the existence of contact structures for energy level sets Σ_c of the mentioned values and small mass ratios of the spatial problem. In the planar case the constructed orbits are noncontractible even in the Moser-regularised energy hypersurface $\bar{\Sigma}_c$. Here, the constructed orbits still obstruct the existence of contact structures in certain relative de Rham classes of $\bar{\Sigma}_c$ to the Liouville 1-form. These results are optimal in the sense that for energies above zero the level sets are again contact for all mass ratios. Numerical results are additionally given to visualise the computations and give evidence for the existence of these orbits for higher mass ratios.

Contents

1	Introduction	2
2	Energy hypersurfaces	5
3	Generating orbits	10
3.1	First species	11
3.2	Second species	11
3.2.1	S-arcs	12
3.2.2	T-arcs	12
3.3	Continuation of second species generating orbits	13
3.3.1	A more general result	13

3.3.2	Application to the restricted three-body problem	15
4	Action of generating orbits	18
4.1	First species	19
4.1.1	First kind	19
4.1.2	Second kind	20
4.2	Second species	21
4.3	Lambert's Theorem	23
4.4	Sequences of generating orbits	26
4.4.1	Fixed semi-minor axis	27
4.4.2	Fixed polar intersection angle with the unit circle	29
5	Proof of main theorem	35
6	Numerical results	40
6.1	First orbit in sequence with varying intersection angle	40
6.2	Sequence at 10 degrees intersection angle	41
	References	50

1 Introduction

In order to use modern mathematical methods, often a contact structure is required. A first step in connecting the restricted three-body problem to Reeb dynamics was done by Albers, Frauenfelder, van Koert and Parternain in [AFvKP12], showing that the bounded components of the Moser-regularised energy hypersurface of the planar restricted three-body problem is of contact type below the first critical energy level and also slightly above this value. The same result for the spatial problem was proven by Cho, Jung and Kim in [CJK20]. Although the spatial case has more physical relevance, for example in space mission design, some results on contact manifolds currently only work for three-dimensional manifolds, e.g. energy level sets inside a four-dimensional phase space of a two-dimensional configuration space. For energies above zero the restricted three-body problem again admits a contact structure as the canonical Liouville 1-form becomes a contact form. This can be checked easily by checking that the corresponding Liouville vector field is transverse to the energy hypersurfaces.

So the question remains: What happens for energies in between these two values? This present work focuses on the region between the highest critical energy value and zero, and the main statements are the following:

Theorem 1.1:

The spatial restricted three-body problem is in general not of contact type for energies between $-\sqrt{2}$ and zero.

Theorem 1.2:

If the planar restricted three-body problem is of contact type between $-\sqrt{2}$ and zero, then the de Rham class of the contact form minus the Liouville 1-form must become infinitely bad for small mass ratios μ .

A more detailed version of the statements can be found in theorem 5.3. In order to explain the result more explicitly, let $(T^*N, d\lambda)$ be the exact symplectic manifold of a cotangent bundle together with the exterior derivative of the canonical Liouville 1-form λ . To define the restricted three-body problem, let μ be the mass ratio of the two primaries M_1 and M_2 . The Hamiltonian is given by

$$H_\mu(q, p) = \frac{1}{2} \left((p_1 + q_2)^2 + (p_2 - q_1)^2 + p_3^2 \right) - \frac{1 - \mu}{\|q - M_1\|} - \frac{\mu}{\|q - M_2\|} - \frac{q_1^2 + q_2^2}{2}, \quad (1)$$

where q are the position coordinates in $\mathbb{R}^3 \setminus \{M_1, M_2\}$ and p are the momentum coordinates in $T_q^*(\mathbb{R}^3 \setminus \{M_1, M_2\})$. The planar case is recovered by setting $q_3 = p_3 = 0$. Dynamics are given by Hamilton's equation of motion and by the conservation of energy, solutions to this Hamiltonian system with energy $H_\mu = c$ stay in their own energy level set $\Sigma_{\mu, c}$ for all time. For all energies the hypersurface $\Sigma_{\mu, c}$ can be regularised at collision with the primaries using the Moser regularisation. We will denote the regularised energy hypersurface by $\bar{\Sigma}_{\mu, c}$. The question is whether one can find a contact structure α on $\bar{\Sigma}_{\mu, c}$ that is compatible with the symplectic structure ω on $T^*(\mathbb{R}^n \setminus \{M_1, M_2\})$ in the sense that $d\alpha = \omega$ and orientations are preserved. If that is the case, the Reeb flow is a positive reparametrisation of the Hamiltonian flow and we can compute the integral of α along a contractible orbit γ by

$$0 < \int \gamma^* \alpha = \int \gamma^* \lambda - \sum \left(r_i \int \gamma^* \beta_i \right),$$

where λ is the canonical Liouville 1-form on the cotangent bundle, β_i are de Rham generators and r_i are the corresponding coefficients of the de Rham class of $\lambda - \alpha$ in $\bar{\Sigma}_c$. The integral $\int \gamma^* \lambda$ is called the action of the orbit. If one now has a contractible periodic orbit with negative action there can not exist a contact structure. The action of noncontractible orbits, on the other hand, only obstructs the existence of contact structures in certain relative de Rham classes.

Over the course of this work we will first compute de Rham generators of the regularised energy hypersurfaces in chapter 2. This is done by analysing the Moser regularisation in the setting of the theorem of Seifert-van Kampen and then applying these relations locally for the restricted three-body problem.

Then we will recall the notion of generating orbits from [Hén97] in chapter 3. In short these generating orbits are limit orbits as $\mu \rightarrow 0$. They turn out to be either orbits of the limit Hamiltonian system, called the *rotating Kepler problem*, or the Kepler problem in

rotating coordinates (q, p) , with its Hamiltonian

$$\begin{aligned} H_0(q, p) &= H_{\text{fix}}(q, p) + L(q, p) \\ &= \frac{\|p\|^2}{2} + q_1 p_2 - q_2 p_1 - \frac{1}{\|q\|} \end{aligned} \quad (2)$$

or pieces of such solutions, glued together at collision with M_2 .

The advantage of working with these generating orbits is that one can now use the Kepler problem

$$H_{\text{fix}}(Q, P) = \frac{1}{2} \|P\|^2 - \frac{1}{\|Q\|}, \quad (3)$$

where we know that solutions are ellipses with focus at the origin with period

$$T = 2\pi\sqrt{a^3}, \quad (4)$$

where a is the semi-major axis of the ellipse. Furthermore, one can recover the Kepler energy H_{fix} and the angular momentum L by

$$H_{\text{fix}} = -\frac{1}{2a} \quad \text{and} \quad (5)$$

$$L = -\epsilon' \sqrt{a(1 - \epsilon^2)}, \quad (6)$$

where ϵ is the eccentricity and ϵ' the direction of rotation defined by

$$\epsilon' := \begin{cases} +1 & \text{for anti-clockwise motion and} \\ -1 & \text{for clockwise motion.} \end{cases} \quad (7)$$

We call the case of $\epsilon' = +1$ *direct* or *prograde motion* and $\epsilon' = -1$ *retrograde*.

This is used in chapter 4 to compute the action of generating orbits and ultimately find sequences of orbits with action tending towards negative values and energy tending to values between $-\sqrt{2}$ and zero. Another main ingredient for this computation is the Levi-Civita regularisation given by the map

$$\begin{aligned} l: \mathbb{C} \setminus \{0\} &\rightarrow \mathbb{C} \setminus \{0\} \\ X &\mapsto X^2 \end{aligned} \quad (8)$$

in complex coordinates $X \in \mathbb{C} \cong \mathbb{R}^2$. This maps solutions for the harmonic oscillator with spring constant $8H_{\text{fix}}$ onto Kepler solutions as a double cover with reparametrisation

$$dt = 4|X|^2 ds \quad (9)$$

between the usual time t and the regularised time s .

The corresponding solutions to the attractive harmonic oscillator are ellipses with

centre at the origin and frequency

$$\varpi = \sqrt{-8H_{\text{fix}}} \quad (10)$$

for negative energies. After rotation and time-shift as in [Cel06] we have solutions

$$X_1(s) = \alpha \cos(\varpi s) \quad X_2(s) = \beta \sin(\varpi s), \quad (11)$$

where we can express the coefficients by

$$\alpha = \sqrt{a(1 + \epsilon)} \quad (12)$$

$$\beta = \epsilon' \sqrt{a(1 - \epsilon)}. \quad (13)$$

As a last ingredient we need the elapsed time of a Keplerian arc from collision to collision, which can be computed using Lambert's theorem and the free-fall time

$$t_{Q_0}(Q_1) = \sqrt{\frac{Q_0^3}{2}} \left(\sqrt{\frac{Q_1}{Q_0} \left(1 - \frac{Q_1}{Q_0} \right)} + \arccos \left(\sqrt{\frac{Q_1}{Q_0}} \right) \right) \quad (14)$$

from height Q_0 down to Q_1 .

Putting all the statements together, we can prove the main theorem in chapter 5. We also add some numerical computations as visualisation and as evidence of how far these orbits survive in terms of mass ratio in the restricted three-body problem. Since all orbits are symmetric with respect to the anti-symplectic involution

$$\rho: (q_1, q_2, q_3, p_1, p_2, p_3) \mapsto (q_1, -q_2, q_3, -p_1, p_2, p_3), \quad (15)$$

they can be found by a perpendicular shooting method.

2 Energy hypersurfaces

The main goal of this chapter is to compute generators of the first de Rham cohomology, which is essential to us for the obstruction to contact forms by closed orbits. These generators are found by computing the fundamental group of the Moser-regularised energy hypersurface, then abelianising it to the first homology group, modding out torsion to get real coefficients and, finally, dualising to get generators of the first de Rham cohomology. We will write all groups that appear here multiplicatively unless they are inherently abelian, in which case we will write them additively. First of all, we will compute the planar case which will take most of this chapter and then comment on the spatial case.

Recall the notation $\Sigma_c := H^{-1}(c)$ for the energy hypersurface of the Kepler problem or the restricted three-body problem. Denote by $\bar{\Sigma}_c$ the corresponding regularised energy hypersurface, where collisions have been added by Moser regularisation. In the first step we compute the fundamental group of $\bar{\Sigma}_c$ using the well-known theorem of Seifert-van Kampen.

We will explicitly compute the fundamental group of the bounded component of the regularised energy hypersurface of the Kepler problem and then use the relations found there to compute the more complicated hypersurface of the restricted three-body problem above the highest critical value $H_\mu(L_5)$.

In the Moser regularisation first the roles of P and Q are interchanged, such that the base points of the cotangent bundle now corresponded to the momentum of the particle and the fibre to its position. At every point in the base the intersection between the hypersurface and the fibre is then a circle of positions. The base as points of momentum is endowed with the metric of the stereographic projection of S^2 through the north pole \mathcal{N} , corresponding to infinite momentum at collision. The regularised energy hypersurface is thus the unit cotangent bundle $S^*(S^2) \cong \mathbb{R}\mathbb{P}^3$ of the round 2-sphere. We choose as the second chart of S^2 the stereographic projection through the south pole \mathcal{S} , corresponding to zero momentum. So, we define the subsets

$$\begin{aligned} U_1 &:= S^*(S^2 \setminus \{\mathcal{N}\}) \cong S(\mathbb{R}^2) \\ U_2 &:= S^*(S^2 \setminus \{\mathcal{S}\}) \cong S(\mathbb{R}^2) \text{ and} \\ U_3 &= S^*(S^2 \setminus \{\mathcal{S}, \mathcal{N}\}) \cong S(\mathbb{R}^2 \setminus \{0\}), \end{aligned}$$

where the trivialisations of U_1 and U_3 are given by the stereographic projection through the north pole and the trivialisation of U_2 by the stereographic projection through the south pole. The change of these variables is given in local coordinates $x \in \mathbb{R}^2$ by

$$\Phi(x_1, x_2) = \left(\frac{x_1}{x_1^2 + x_2^2}, \frac{x_2}{x_1^2 + x_2^2} \right)$$

and the Jaconian is

$$\mathrm{D}\Phi(x_1, x_2) = \frac{1}{(x_1^2 + x_2^2)^2} \begin{pmatrix} x_2^2 - x_1^2 & -2x_1x_2 \\ -2x_1x_2 & x_1^2 - x_2^2 \end{pmatrix}.$$

As the base point for the fundamental groups we choose

$$x_0 := ((1, 0), (1, 0)) \in S(\mathbb{R}^2 \setminus \{0\}) \cong U_3 = U_1 \cap U_2,$$

i. e. the point with momentum $P = (1, 0)$ and position $Q = (1, 0)$. In the trivialisation of U_2 this point x_0 corresponds to $((1, 0), (-1, 0)) \in S(\mathbb{R}^2)$.

The fundamental groups of the subsets are

$$\begin{aligned} \pi_1(U_1, x_0) &= \langle \zeta \rangle \cong \mathbb{Z} \\ \pi_1(U_2, x_0) &= \langle \eta \rangle \cong \mathbb{Z} \\ \pi_1(U_3, x_0) &= \langle \xi_1, \xi_2 \mid [\xi_1, \xi_2] \rangle \cong \mathbb{Z} \times \mathbb{Z}, \end{aligned}$$

where ζ and ξ_1 is each the class of homotopic loops based at x_0 and represented by

$$t \mapsto ((1, 0), (\cos(2\pi t), \sin(2\pi t))),$$

i. e. a simple loop in the position fibre, η is also represented by a loop

$$t \mapsto ((1, 0), (-\cos(2\pi t), \sin(2\pi t))),$$

in the fibre and ξ_2 is represented by a loop

$$t \mapsto ((\cos(2\pi t), \sin(2\pi t)), (1, 0))$$

in the momentum base.

For the theorem of Seifert-van Kampen we need to compute the images $v_i(\xi_j)$ for $i, j \in \{1, 2\}$ of generators of $\pi_1(U_3, x_0)$ after the homomorphisms v_i induced by the inclusions $U_i \hookrightarrow U_3$. Since we chose the same trivialisation for U_1 and U_3 , the first two are simply $v_1(\xi_1) = \zeta$ and $v_1(\xi_2) = 1$ because ζ and ξ_1 are identically represented in the trivialisation and the representation of ξ_2 is contractible in U_1 . For the second homomorphism v_2 we need to check the differential of the change of trivialisations, i. e. the Jacobian of the change of coordinates between the stereographic projection through the north and the south pole.

The representation of ξ_1 readily gets mapped onto the representation of η , so $v_2(\xi_1) = \eta$. The image of the representation of ξ_2 is again contractible in the base, but it twists the fibre twice in the opposite direction of η since

$$\begin{aligned} D\Phi(\cos(2\pi t), \sin(2\pi t)) \begin{pmatrix} 1 \\ 0 \end{pmatrix} &= (\sin^2(2\pi t) - \cos^2(2\pi t), -2\sin(2\pi t)\cos(2\pi t)) \\ &= (-\cos(4\pi t), -\sin(4\pi t)). \end{aligned}$$

All in all we have

$$\begin{aligned} v_1(\xi_1) &= \zeta, & v_1(\xi_2) &= 1, \\ v_2(\xi_1) &= \eta, & v_2(\xi_2) &= \eta^{-2} \end{aligned}$$

and the fundamental group of $\overline{\Sigma}_c$ becomes

$$\pi_1(\overline{\Sigma}_c, x_0) = \langle \zeta, \eta \mid \zeta = \eta, \eta^{-2} \rangle = \langle \zeta \mid \zeta^2 \rangle \cong \mathbb{Z}_2.$$

Of course we would have known that earlier from the fact that $\overline{\Sigma}_c \cong S^*S^2 \cong \mathbb{RP}^3$, but now we can use the relations from above to compute the fundamental groups of more complicated regularised hypersurfaces.

The surface we are interested in is the energy level set of the restricted three-body problem above the highest critical value $H_\mu(L_5) < c$. Here, we need to regularise two singularities and we will therefore apply the theorem of Seifert-van Kampen twice. As the subsets we again choose the unregularised energy level set

$$U_1 := \Sigma_c \cong S^*(\mathbb{R}^2 \setminus \{M_1, M_2\}) \cong S(\mathbb{R}^2 \setminus \{M_1, M_2\}),$$

for the local regularising charts each a copy of the unit cotangent bundle of a small open

2-disc

$$U_2, U_3 := S^*(B_\varepsilon) \cong S(\mathbb{R}^2),$$

and the intersections become unit cotangent bundles of punctured 2-discs

$$U_4, U_5 := S^*(B_\varepsilon \setminus \{0\}) \cong S(\mathbb{R}^2 \setminus \{0\}).$$

Remember, however, that the trivialisation of Σ_c , where currently the position coordinates form the base, is changed in the first step of regularisation, such that the momentum becomes the base and the fibre is the position. The fundamental groups of these spaces are

$$\begin{aligned}\pi_1(U_1) &= \langle r, w_1, w_2 \mid [r, w_1], [r, w_2] \rangle, \\ \pi_1(U_2) &= \langle \eta_2 \rangle, \\ \pi_1(U_3) &= \langle \eta_3 \rangle, \\ \pi_1(U_4) &= \langle \xi_1, \xi_2 \mid [\xi_1, \xi_2] \rangle \quad \text{and} \\ \pi_1(U_5) &= \langle \xi_3, \xi_4 \mid [\xi_3, \xi_4] \rangle,\end{aligned}$$

where r is represented by the loop in momentum coordinates over a fixed position, w_1 is the winding in position around M_1 and w_2 is the winding in position around M_2 , both commuting with r . The two η_2 and η_3 are defined, same as η above, as the loop in position coordinates, as well as ξ_1 and ξ_3 , just as in ξ_1 from above, while ξ_2 and ξ_4 are a represented by a loop in momentum coordinates, as was ξ_2 from before. Denote the homomorphisms of fundamental groups induced by inclusions as

$$\begin{aligned}v_1: \pi_1(U_4) &\rightarrow \pi_1(U_1), & v_3: \pi_1(U_5) &\rightarrow \pi_1(U_1), \\ v_2: \pi_1(U_4) &\rightarrow \pi_1(U_2), & v_4: \pi_1(U_5) &\rightarrow \pi_1(U_3).\end{aligned}$$

We can now use the same relations as in the Kepler problem:

$$\begin{aligned}v_1(\xi_1) &= w_1 & v_1(\xi_2) &= r \\ v_2(\xi_1) &= \eta_2 & v_2(\xi_2) &= \eta_2^{-2} \\ v_3(\xi_3) &= w_2 & v_3(\xi_4) &= r \\ v_4(\xi_3) &= \eta_3 & v_4(\xi_4) &= \eta_3^{-2}\end{aligned}$$

The only difference is that the loop in momentum coordinates is no longer contractible in the original $\Sigma_c = U_1$. Putting together the generators and relations, we get

$$\begin{aligned}\pi_1(\overline{\Sigma}_c) &= \langle r, w_1, w_2, \eta_2, \eta_3 \mid [r, w_1], [r, w_2], w_1 = \eta_2, r = \eta_2^{-2}, w_2 = \eta_3, r = \eta_3^{-2} \rangle \\ &= \langle r, w_1, w_2 \mid [r, w_1], [r, w_2], r = w_1^{-2}, r = w_2^{-2} \rangle \\ &= \langle w_1, w_2 \mid w_1^2 = w_2^2 \rangle.\end{aligned} \tag{16}$$

In order to find the first de Rham cohomology, we first compute the abelianisation

$$\begin{aligned}
H_1(\overline{\Sigma}_c, \mathbb{Z}) &\cong \pi_1(\overline{\Sigma}_c)^{\text{ab}} = \langle w_1, w_2 \mid 2w_1 = 2w_2 \rangle \\
&= \langle w_1, w_2, z \mid 2w_1 = 2w_2, z = w_2 - w_1 \rangle \\
&= \langle w_1, z \mid 2z \rangle \\
&\cong \mathbb{Z} \times \mathbb{Z}_2,
\end{aligned}$$

which is isomorphic to the first homology group with integer coefficients. By modding out torsion by the universal coefficient theorem we get the first homology with real coefficients

$$H_1(\overline{\Sigma}_c, \mathbb{R}) \cong \mathbb{R} \cong H_{\text{dR}}^1(\overline{\Sigma}_c),$$

which is also isomorphic to the first de Rham cohomology by duality and de Rham's theorem. We denote the push forward of the inclusion $\iota: \Sigma_c \hookrightarrow \overline{\Sigma}_c$ on homology by

$$\iota_*: H_1(\Sigma_c) \cong \mathbb{R}^3 \rightarrow H_1(\overline{\Sigma}_c) \cong \mathbb{R}.$$

The kernel of ι_* can be found from line (16) to be $\ker(\iota_*) = \langle r + 2w_1, r + 2w_2 \rangle_{\mathbb{R}}$ and the coimage is then $\ker(\iota_*)^\perp = \langle 2r - w_1 - w_2 \rangle_{\mathbb{R}}$, where we abuse the notation from above of fundamental classes r, w_1 and w_2 to also denote generators of homology.

Dualising to cohomology, we see that the image of the pullback of ι on cohomology

$$\iota^*: H_{\text{dR}}^1(\overline{\Sigma}_c) \cong \mathbb{R} \rightarrow H_{\text{dR}}^1(\Sigma_c) \cong \mathbb{R}^3$$

is then $\text{im}(\iota^*) = \langle 2d\vartheta - d\varphi_1 - d\varphi_2 \rangle$, where ϑ is the polar angle in momentum coordinates and φ_1 and φ_2 are polar angles in position coordinates centred at M_1 and M_2 , respectively. So, we have found a generator of the first de Rham cohomology of the regularised energy hypersurface above the highest critical value, which we can compute easily for periodic non-collision orbits by twice the rotation number minus the two winding numbers around the primaries. We summarise the results from this chapter on the planar restricted three-body problem in the following lemma:

Lemma 2.1:

For the planar circular restricted three-body problem and energies c above the highest critical value $H_\mu(L_5)$ the first de Rham cohomology of the Moser-regularised energy hypersurface $\overline{\Sigma}_c$ is one-dimensional and has generator $0 \neq [\beta_0] \in H_{\text{dR}}^1(\overline{\Sigma}_c)$ which agrees with $2d\vartheta - d\varphi_1 - d\varphi_2$ on the unregularised level set Σ_c .

If we use the same setup in the spatial case, we see that all sets

$$\begin{aligned}
U_1 &= \Sigma_c \cong S(\mathbb{R}^2 \setminus \{M_1, M_2\}), \\
U_2, U_3 &= S^*(B_\varepsilon) \cong S(\mathbb{R}^2) \text{ and} \\
U_4, U_5 &= S^*(B_\varepsilon \setminus \{0\}) \cong S(\mathbb{R}^2 \setminus \{0\})
\end{aligned}$$

are simply connected. Consequently, by the theorem of Seifert-van Kampen also the

union $\overline{\Sigma}_c$ is simply connected. This means that in the spatial restricted three-body problem every closed orbit is contractible in the regularised as well as in the unregularised energy level set.

3 Generating orbits

Next, we will describe the notion of generating orbits for the restricted three-body problem. We will introduce notation but also describe some results from other authors and connect their results to our purposes.

Generating orbits are limits of orbits of the restricted three-body problem. In our setting we will use the limit as $\mu \rightarrow 0$ but in general also other limits, for example letting the angular momentum tend to zero, might be possible. This chapter establishes terminology and results around these generating orbits which is taken from [Hén97]. Another extensive work on generating orbits is [Bru94], where more theory is explained and mainly rotating coordinates are used. In [Hén97] fixed coordinates are used to describe the generating orbits which makes it easier for us to use the geometry of Kepler ellipses and compute the action of generating orbits. We are only interested in periodic orbits here and, hence, we will only consider periodic generating orbits.

Definition 3.1:

Let γ_μ be a periodic orbit of the restricted three-body problem with mass ratio $\mu > 0$. Then γ is called a *generating orbit* if there exists a sequence of orbits γ_μ such that $\gamma_\mu \rightarrow \gamma$ as $\mu \rightarrow 0$.

Remark 3.2:

In general, generating orbits are not orbits of the restricted three-body problem for $\mu = 0$, i. e. the rotating Kepler problem, and vice-versa. Furthermore, when we use the notion of a generating orbit, we usually mean this in Henon's terms, who mostly worked with numerical methods. For an analytical proof of the fact that there exist continued orbits in the restricted three-body problem we rely on section 3.3.

Next, we will classify *species* of generating orbits. This notion goes back to Poincaré in [Poi99] who called his predicted periodic orbits with near collisions in the general three-body problem “solutions périodiques de deuxième espèce”. We will adopt Hénon's more general definition of orbit species:

Definition 3.3:

A generating orbit is of the *first species* if it is a Keplerian orbit, it is of the *second species* if at least one point coincides with M_2 and it is of the *third species* if it only consists of M_2 .

This definition does not give mutually exclusive species. In fact, third species generating orbits are always also of both the first and the second species. There are second species orbits that are also of the first species but there are also orbits that are exclusively of the first or second species. However, this definition is in terms of Hénon's *principle of*

positive definition where “a definition relating to orbits in a family should not be based on a negative property, such as an inequality”. This principle gives families of generating orbits the same species at the cost of exclusivity of species.

3.1 First species

First species orbits are periodic orbits of the rotating Kepler problem. We define in accordance with the principle of positive definition:

Definition 3.4:

A generating orbit of the first species is called of the *first kind* if it is a circular orbit and of the *second kind* if in fixed coordinates M_2 and M_3 each make an integral number of revolutions I and J around M_1 .

Again, this definition is not exclusive and orbits belonging to both kinds are bifurcation orbits. More details on the first species can be found in [Hén97].

3.2 Second species

According to definition 3.3 a second species orbit passes through M_2 at least once. We call this event a *collision*. A periodic second species generating orbit will collide infinitely many times, but there can also be multiple collisions during one minimal period. Abiding by the principle of positive definition, we declare a finite piece of a Keplerian orbit which begins and ends in collision an *arc*. Note that also an arc can include collisions, subdividing the arc into *basic arcs*. The angle at collision between basic arcs is called the *deflection angle* and a generating orbit of the second species is called *ordinary generating orbit* if all deflection angles are nonzero. Non-ordinary generating orbits are again bifurcation orbits.

The Kepler orbit belonging to the arc is called the *supporting Kepler orbit* or the *supporting Kepler ellipse*, if referring to the geometrical object. Each second species generating orbit consists of a sequence of arcs U_1, U_2, \dots, U_k , which is repeated periodically, and each arc is fully defined by its supporting Kepler solution and times t'_j and t''_j of initial and final collision. The *duration* of an arc U_j is $\tau_j := t''_j - t'_j$.

The further study of second species orbits will from now on be confined to the study of arcs where we will continue to only state results and definitions which we will work with later.

Let r_1 be the pericentre distance and r_2 the apocentre distance of the supporting ellipse. For a collision to occur, we need $r_1 \leq 1 \leq r_2$. We will distinguish the following cases: For $r_1 < 1 < r_2$ we have a non-circular supporting ellipse which intersects the unit circle in two distinct points transversally. The corresponding arcs will be called of *type 1*. For $r_1 = 1$ and $r_2 > 1$ or $r_1 < 1$ and $r_2 = 1$ the supporting Kepler ellipse is tangent to the unit circle and we will call the arcs of *type 2*. In the remaining case $r_1 = r_2 = 1$ the supporting Kepler ellipse is identical with the unit circle and we will call the corresponding arc of *type 3* if it is retrograde and of *type 4* if it is direct. Type 1 is the most interesting and comes in families while the other types are isolated.

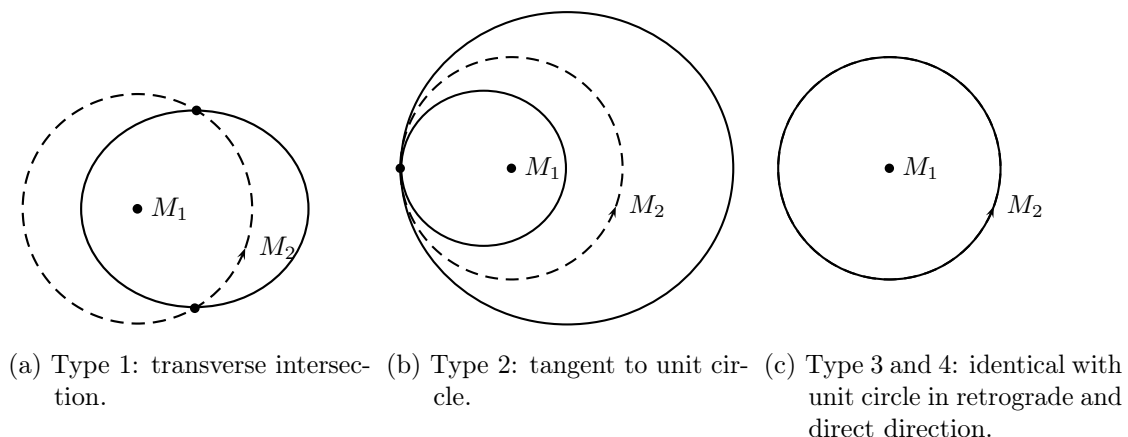


Figure 1: Types of second species supporting ellipses.

We will further subdivide type 1 arcs into *S-arcs* which in fixed coordinates begin and end at different points on the unit circle and *T-arcs* which begin and end at the same point. A type 1 arc will furthermore be called *ingoing* if at the initial collision its velocity vector points to the inside of the unit circle, and *outgoing* else. Both *S-arcs* and *T-arcs* can be ingoing and outgoing.

3.2.1 S-arcs

An *S*-arc is symmetric with respect to the major axis of the supporting ellipse in fixed coordinates and intersects this axis $2J + 1$ times for $J \geq 0$. Let R be the central—i. e. the $J + 1^{\text{st}}$ —intersection point. Then R lies either at the pericentre or apocentre and we call it the *midpoint*. Since both collision points lie at $(1, 0)$ in rotating coordinates, the midpoint R also lies on the q_1 -axis and the arc is symmetric with respect to ρ from (15).

3.2.2 T-arcs

T-arcs begin and end in the same point in fixed coordinates and are therefore full Kepler ellipses. Analogously to rotating Kepler orbits, the semi-major axis of the supporting ellipse can be expressed by numbers I and J of rotation of M_2 and M_3 around M_1 by $a = (I/J)^{2/3}$. Because we have

Proposition 3.5 (proposition 4.3.2 in [Hén97]):

An ordinary generating orbit of the second species can not contain two identical T-arcs of type 1 in succession.

the numbers I and J must again be relatively prime, i. e. no multiple covers are allowed. *T*-arcs are not symmetric and for every mutually prime I and J there exists a family $T_{I,J}^i$ of ingoing *T*-arcs and a family $T_{I,J}^e$ of outgoing *T*-arcs.

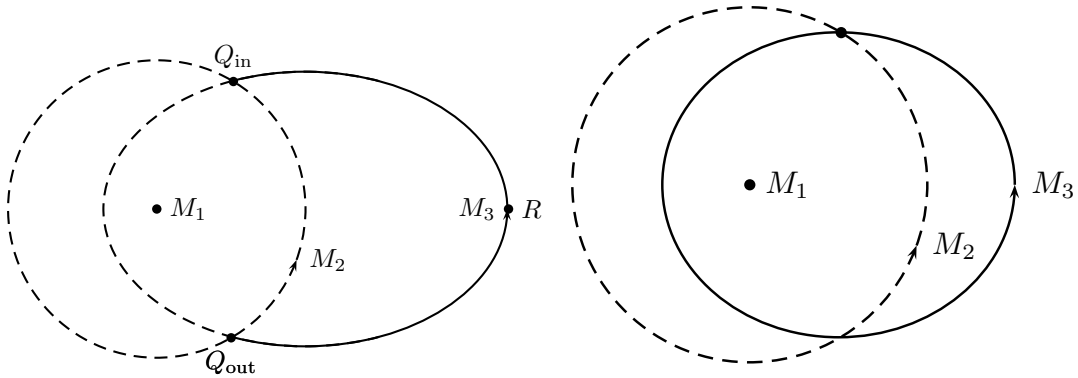


Figure 2: An outgoing S-arc and an ingoing T-arc.

3.3 Continuation of second species generating orbits

In order to show analytically that the orbits described above are actually generating orbits we need to find converging sequences of orbits in the restricted three-body problem as $\mu \rightarrow 0$. Conversely, we then have for every generating orbit an arbitrarily close orbit in the restricted problem for some small enough mass ratio.

For first species orbits there are many works on the existence of such sequences, for example [Poi92], [Bir14] and [Hag70] for the first kind, [Are63] for symmetric, and [Bru94] for asymmetric second kind orbits. The remainder of this chapter is focused on second species generating orbits.

3.3.1 A more general result

The main theorem from [BM00] helps to show that many ordinary second species orbits are actually generating orbits. The setting is somewhat more general in that paper and we can also follow from the proof presented there that the action of the orbits in the restricted three-body problem converges to the action of the generating orbit. We will therefore first describe the notation which we adapt for our purposes and then explain in more detail the result and the relevance for the present work.

Let \mathcal{Q} be a two- or three-dimensional smooth manifold and $\mathcal{P} = \{p_1, \dots, p_n\} \subset \mathcal{Q}$ a finite subset. The set $\mathcal{Q} \setminus \mathcal{P}$ shall be the configuration space for the Hamiltonian

$$H_\mu(q, p) = H_0(q, p) + \mu V(q),$$

where $H_0(q, p) = \frac{1}{2} \|p + A_q\|_{g_q^*}^2 + W(q)$ is a magnetic Hamiltonian and V is another smooth potential with Newtonian singularities at every $p_i \in \mathcal{P}$. So, the Hamiltonian H_0 is defined on all of $T^*\mathcal{Q}$, while H_μ is defined on $T^*(\mathcal{Q} \setminus \mathcal{P})$. For the planar restricted three-body problem with small mass ratio μ we choose $\mathcal{Q} = \mathbb{R}^2 \setminus \{0\}$ and $\mathcal{P} = \{(1, 0)\}$, i. e. we shift the coordinates such that the origin is always at the heavier primary M_1 .

The Hamiltonian then is of the form from above, with

$$A_q = q_2 dq_1 - q_1 dq_2,$$

$$W(q) = -\frac{1}{\|q\|} - \frac{\|q^2\|}{2} \quad \text{and} \quad V(q) = \frac{1}{\|q\|} - \frac{1}{\|q - (1, 0)\|} - q_1.$$

Fix an energy c such that the open Hill's region $\mathfrak{H}_c := \{q \in \mathcal{Q} \mid W(q) < c\}$ contains \mathcal{P} . Suppose we have a finite set K of nondegenerate collision orbits $\gamma_k: [0, \tau_k] \rightarrow \mathfrak{H}_c$ of the Hamiltonian system H_0 such that $\gamma_k(0) = p_{\alpha_k}$, $\gamma_k(\tau_k) = p_{\beta_k} \in \mathcal{P}$ and $\gamma(t) \in \mathfrak{H}_c \setminus \mathcal{P}$ for all other $t \in (0, \tau_k)$. A *chain* is a sequence $(\gamma_{k_i})_{i \in \mathbb{Z}}$ of orbits in K such that additionally $\gamma_{k_i}(\tau_{k_i}) = \gamma_{k_{i+1}}(0)$ and $\dot{\gamma}_{k_i}(\tau_{k_i}) \neq \dot{\gamma}_{k_{i+1}}(0)$, i. e. they are connected collision orbits with nonzero deflection angle. Let \mathcal{W}_k be open neighbourhoods for each of the sets $\gamma_k([0, \tau_k])$ in \mathcal{Q} . An orbit $\gamma: \mathbb{R} \rightarrow \mathfrak{H}_c$ is said to *shadow* the chain $(\gamma_{k_i})_{i \in \mathbb{Z}}$ if there exists an increasing sequence $(t_i)_{i \in \mathbb{Z}}$ such that $\gamma([t_i, t_{i+1}]) \subset \mathcal{W}_{k_i}$.

The *nondegeneracy* of such orbits γ is defined as the Morse-nondegeneracy of the critical point $(u, \tau) \in W^{1,2}(p_\alpha, p_\beta) \times \mathbb{R}^+$ of the action functional $\mathcal{A}(\gamma)$, where $W^{1,2}(p_\alpha, p_\beta)$ is the space of all $W^{1,2}$ -functions $u: [0, 1] \rightarrow \mathcal{Q}$ with fixed endpoints $u(0) = p_\alpha$, $u(1) = p_\beta$ and $\gamma(t) = u(t/\tau)$. There are four other equivalent ways to define the nondegeneracy described in [BM00]. The only other one we will use here is the following: Denote by $q(\lambda, t)$ the general solution of Hamilton's second order differential equations of motion in the configuration space with parameter λ and by $h(\lambda)$ the Hamiltonian energy. Then the collision orbit is nondegenerate if the system

$$q(\lambda, 0) = p_\alpha, \quad q(\lambda, \tau) = p_\beta, \quad h(\lambda) = c \tag{17}$$

has full rank $2 \dim \mathcal{Q} + 1$.

Theorem 3.6 (theorem 1.1 from [BM00]):

There exists $\mu_0 > 0$ such that for all $\mu \in (0, \mu_0]$ and any chain $(\gamma_{k_i})_{i \in \mathbb{Z}}$ the following holds:

- *There exists a trajectory $\gamma: \mathbb{R} \rightarrow \mathfrak{H}_c$ of energy c for the system H_μ shadowing the chain $(\gamma_{k_i})_{i \in \mathbb{Z}}$ and it is unique up to a time-shift if the neighbourhoods \mathcal{W}_k are chosen small enough.*
- *The orbit γ converges to the chain of collision orbits as $\mu \rightarrow 0$: There exists an increasing sequence $(t_i)_{i \in \mathbb{Z}}$ such that*

$$\max_{t_i \leq t \leq t_{i+1}} \text{dist}(\gamma(t), \gamma_{k_i}([0, \tau_{k_i}])) \leq \mu C_1,$$

where the constant $C_1 > 0$ depends only on the set K of collision orbits.

- *If we additionally have $\dot{\gamma}_{k_i}(\tau_{k_i}) \neq -\dot{\gamma}_{k_{i+1}}(0)$, the orbit γ avoids collision by a distance of order μ : there exists a constant $C_2 \in (0, C_1)$, depending only on K , such that*

$$\mu C_2 \leq \min_{t_{i-1} \leq t \leq t_{i+1}} \text{dist}(\gamma(t), p_{\alpha_{k_i}}).$$

3.3.2 Application to the restricted three-body problem

We now want to apply this theorem 3.6 to the restricted three-body problem and find orbits for positive mass ratios $\mu > 0$ shadowing chains of collision orbits, i. e. second species generating orbits. In the same paper [BM00] a partial result is already shown:

Lemma 3.7 (lemma 3.2 in [BM00]):

For $c \in (-3/2, \sqrt{2})$ the collision orbit at $\mu = 0$ in the rotating frame corresponding to a whole number I of revolutions of an ellipse with rational frequency $I/J \in A_c$ in the allowed set of frequencies A_c for energy c starting and ending at a collision with M_2 is nondegenerate.

In the language of generating orbits this means that every ordinary generating orbit composed of T-arcs is indeed a generating orbit. We would like to use generating orbits composed of S-arcs and we will therefore have to prove accordingly:

Lemma 3.8:

For $c \in (-3/2, \sqrt{2})$ a non-rectilinear ordinary S-arc collision orbit starting and ending in M_2 with semi-major axis $a > 1$ of the supporting ellipse is nondegenerate.

Proof: This proof is very similar to the proof of lemma 3.7 in [BM00] but a lot harder to actually compute the estimates. Enforcing the first equation of (17), we have $\dim \mathcal{Q} = 2$ free parameters left for λ . We parametrize the supporting ellipse through our initial point of collision Q_0 by the position of the second focus $F \in \mathbb{R}^2$ using two variables: the polar angle θ between Q_0 and F and the semi-major axis

$$\begin{aligned} a &= \frac{1}{2}(1 + \text{dist}(Q_0, F)) \\ &= \frac{1}{2}(1 + \sqrt{1 + \text{dist}(M_1, F)^2 - 2 \cos(\theta) \text{dist}(M_1, F)}). \end{aligned}$$

This is a good parameter if $\text{dist}(M_1, F) \neq \cos \theta$ or, equivalently, if $\text{dist}(Q_0, F) \neq \sin \theta$, so we restrict to $\text{dist}(Q_0, F) > 1$, i. e. if and only if $a > 1$. We will see later on that this does effectively not restrict S-arcs in the direct sense of rotation $\epsilon' = +1$, which are the only ones we need in the main proof.

The second condition of (17) is satisfied nondegenerately since the supporting ellipse intersects the unit circle transversely and both M_2 and M_3 have nonzero velocities. Fixing the endpoint also fixes the angle θ , so the remaining free parameter is a .

We are left to show that the derivative of the energy by a is nonzero. Dependent on a and θ we compute the eccentricity and the energy, as will be also done in section 4.4.2 later on:

$$\begin{aligned} \epsilon &= \frac{\cos \theta + \sqrt{4a^2 - 4a + \cos^2 \theta}}{2a} \\ H_0 &= -\frac{1}{2a} - \epsilon' \sqrt{1 - \cos \theta \frac{\cos \theta + \sqrt{4a^2 - 4a + \cos^2 \theta}}{2a}} \end{aligned}$$

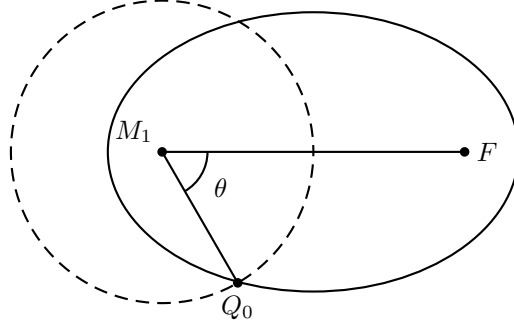


Figure 3: Parametrisation of second species ellipses.

We exclude the case of rectilinear orbits with $\theta = 0$ due to the root being zero and the sign of ϵ' changing here. For numbers of revolution $J > 0$ there would also occur a collision with M_3 and M_1 in that case which one would have to deal with additionally.

For all other orbits with $\theta \in (0, \pi)$ and $a > 1$ we differentiate H_0 by a to get

$$\frac{\partial H_0}{\partial a} = \frac{1}{2a^2} + \epsilon' \frac{\cos \theta \frac{\frac{4a^2-2a}{\sqrt{4a^2-4a+\cos^2\theta}} - \cos \theta - \sqrt{4a^2-4a+\cos^2\theta}}{2a^2}}{2\sqrt{1 - \cos \theta \frac{\cos \theta + \sqrt{4a^2-4a+\cos^2\theta}}{2a}}}.$$

This vanishes if and only if

$$\begin{aligned} 2\sqrt{1 - \cos \theta \frac{\cos \theta + \sqrt{4a^2 - 4a + \cos^2 \theta}}{2a}} &= \\ &= -\epsilon' \cos \theta \left(\frac{4a^2 - 2a}{\sqrt{4a^2 - 4a + \cos^2 \theta}} - \cos \theta - \sqrt{4a^2 - 4a + \cos^2 \theta} \right) \\ &= \frac{-2\epsilon' a \cos \theta}{\sqrt{4a^2 - 4a + \cos^2 \theta}} \underbrace{\left(1 - \cos \theta \frac{\cos \theta + \sqrt{4a^2 - 4a + \cos^2 \theta}}{2a} \right)}_{=a(1-\epsilon^2)>0}. \end{aligned}$$

Based on this equation, we can distinguish four cases: Case 1 is $\epsilon' = +1$ and $\cos \theta \geq 0$, case 2 is $\epsilon' = +1$ and $\cos \theta < 0$, case 3 is $\epsilon' = -1$ and $\cos \theta > 0$, and case 4 is $\epsilon' = -1$ and $\cos \theta \leq 0$.

In cases 1 and 4 the right-hand side becomes nonpositive and the nondegeneracy is obvious since the left-hand side is always positive for $\epsilon \neq 1$. For the remaining cases we will have to work a little bit harder. In the following computations we will denote the left-hand side by $u = u(a, \theta)$ and the right-hand side by $v = v(a, \theta)$.

In case 2 the sign of $\cos \theta$ is negative, so we can estimate the left-hand side by $u > 2$.

To show that the right-hand side v is smaller, we insert the boundary value $a = 1$ to get

$$v(1, \theta) = \frac{-2 \cos \theta}{|\cos \theta|} (1 - \cos \theta (\cos \theta + |\cos \theta|)) = 2$$

and then see that the derivate $\partial v / \partial a$ is negative by

$$\begin{aligned} \frac{\partial v}{\partial a} &= \\ -\cos \theta &\left(\frac{(8a-2)\sqrt{4a^2-4a+\cos^2\theta} - (4a^2-2a)\frac{8a-4}{2\sqrt{4a^2-4a+\cos^2\theta}}}{4a^2-4a+\cos^2\theta} - \frac{8a-4}{2\sqrt{4a^2-4a+\cos^2\theta}} \right) \\ &= -\cos \theta \frac{4a \cos^2 \theta - 4a}{(4a^2 - 4a + \cos^2 \theta)^{\frac{3}{2}}} < 0. \end{aligned}$$

In the last remaining case 3 we have $\cos \theta > 0$ and $\epsilon' = -1$, so we can estimate the root in the left-hand side from below to get

$$u(a, \theta) > 2 \left(1 - \cos \theta \frac{\cos \theta + \sqrt{4a^2 - 4a + \cos^2 \theta}}{2a} \right).$$

Therefore, $u > v$ reduces to

$$\begin{aligned} 2 &> \frac{2a \cos \theta}{\sqrt{4a^2 - 4a + \cos^2 \theta}} && \iff \\ 4a^2 - 4a + \cos^2 \theta &> a^2 \cos^2 \theta && \iff \\ (a-1)(a(4 - \cos^2 \theta) - \cos^2 \theta) &> 0 \end{aligned}$$

which is obviously true due to $a > 1$. □

Briefly summarizing this section with focus on the information relevant for the main proof in chapter 5, we can state the following:

Corollary 3.9:

Let γ be an ordinary second species generating orbit with action $\mathcal{A}(\gamma)$ composed of S -arcs and T -arcs with energy $c \in (-3/2, \sqrt{2})$ where all supporting ellipses are non-rectilinear and S -arcs have semi-major axes $a > 1$. Then there exists an $\varepsilon > 0$ and $\mu_0 > 0$ such that for all $\mu \in (0, \mu_0]$ there exists a unique periodic orbit γ_μ with energy c in the restricted three-body problem with mass ratio μ shadowing γ with action $|\mathcal{A}(\gamma_\mu) - \mathcal{A}(\gamma)| < \varepsilon$.

Backed by this result, we will in the next chapter compute the action of generating orbits in order to construct orbits with negative action in the restricted three-body problem with positive mass ratio $\mu \in (0, 1)$.

4 Action of generating orbits

In this chapter we compute the action of first and second species generating orbits for the restricted three-body problem. The first two sections will focus on general formulae for the action of the two species, while the third section will provide a helpful method to compute the elapsed time of second species arcs. Finally, in the last section we construct sequences of second species generating orbits that have special properties with respect to their action and energy. First of all however, we will recall the formula for the action and convert to fixed coordinates (Q, P) in order to subsequently use the geometry of Kepler orbits.

Let $\gamma: S^1 \rightarrow \Sigma_c$ be a nonconstant periodic orbit of the planar restricted three-body problem with period $\tau > 0$ and energy $H_\mu = c$. In rotating coordinates

$$\begin{pmatrix} q_1 \\ q_2 \\ q_3 \end{pmatrix} = \begin{pmatrix} \cos(t) & \sin(t) & 0 \\ -\sin(t) & \cos(t) & 0 \\ 0 & 0 & 1 \end{pmatrix} \begin{pmatrix} Q_1 \\ Q_2 \\ Q_3 \end{pmatrix}$$

we have the action

$$\begin{aligned} \mathcal{A}(\gamma) &:= \int_{S^1} \gamma^* \lambda \\ &= \int_0^\tau p_1(t) \frac{dq_1(t)}{dt} + p_2(t) \frac{dq_2(t)}{dt} dt \\ &= \int_0^\tau p_1(t) (p_1(t) + q_2(t)) + p_2(t) (p_2(t) - q_1(t)) dt \\ &= \int_0^\tau \|p(t)\|^2 + L(t) dt, \end{aligned} \tag{18}$$

where $L(t)$ is the angular momentum $p_1(t)q_2(t) - p_2(t)q_1(t)$. Using fixed coordinates (Q, P) allows us to use all our knowledge about Kepler orbits for our generating orbits. Since both $\|p\|^2$ and $L(t)$ are invariant under the rotation that defines the transformation between fixed and rotating coordinates, the action can simply be written as

$$\mathcal{A}(\gamma) = \int_0^\tau \|P(t)\|^2 + L(t) dt.$$

Solving the Kepler Hamiltonian (3) for $\|P\|^2$ and inserting, we are left with

$$\mathcal{A}(\gamma) = \int_0^\tau 2H_{\text{fix}}(t) + L(t) + \frac{2}{\|Q(t)\|} dt. \tag{19}$$

While for general orbits of the restricted three-body problem the Kepler energy H_{fix} , angular momentum L and distance to the origin $\|Q\|$ all depend on time, at least H_{fix} and L are integrals of motion for the limit case $\mu = 0$. Since generating orbits are merely rotating Kepler ellipses or sequences of Keplerian arcs, we can now quite easily compute

their action. To further get rid of the term $2/\|Q\|$, we apply the change of variables to the regularised time (9) of the Levi-Civita transformation. Ultimately, we get that the action of a generating orbit γ which consists of only one Keplerian arc can be computed by

$$\begin{aligned}\mathcal{A}(\gamma) &= \tau(2H_{\text{fix}} + L) + \int_0^\sigma \frac{2}{\|X\|^2} 4X^2 ds \\ &= \tau(2H_{\text{fix}} + L) + 8\sigma,\end{aligned}\tag{20}$$

where $\sigma = s(\tau)$ is the duration of the arc in Levi-Civita-regularised time. For generating orbits composed of multiple arcs both H_{fix} and L can change between arcs while the relevant energy $H_0 = H_{\text{fix}} + L$ must remain the same. The total action can simply be computed by adding up the actions of all arcs.

4.1 First species

We first compute the action for generating orbits of the first species, i. e. when the orbit is just a full rotating Kepler orbit. One has to keep in mind, however, that the notion of periodicity remains that from the rotating setting.

4.1.1 First kind

For the first kind—circular orbits—the computation is quite easy. One only has to compute the period, which in general differs from the Kepler period.

For circular orbits, additionally to the conserved quantities H_{fix} and L , also the radius $\|Q\|$ is conserved. This means that the integrand of (19) itself is a conserved quantity and integration is merely a multiplication with the period:

$$\mathcal{A}(\gamma) = \tau \left(2H_{\text{fix}} + L + \frac{2}{\|Q\|} \right)\tag{21}$$

Using the computation of the angular velocity $n := 2\pi\epsilon'/T = \epsilon'/\sqrt{a^3}$ in fixed coordinates, the mean motion is decreased by the rotation of the coordinate axes to give an angular velocity of $n - 1 = \epsilon'/\sqrt{a^3} - 1$. The period of circular orbits in the rotating frame is hence

$$\tau = \left| \frac{2\pi}{\frac{\epsilon'}{\sqrt{a^3}} - 1} \right| = \left| \frac{2\pi}{\frac{1}{\sqrt{a^3}} - \epsilon'} \right|.\tag{22}$$

Using equations (5) and (6) for the Kepler energy and angular momentum from the data of the ellipse, we get the action of circular orbits in rotating coordinates as a function of

the semi-major axis a and direction of rotation ϵ' :

$$\begin{aligned}\mathcal{A}(\gamma) &= \frac{2\pi}{\left|\frac{1}{\sqrt{a^3}} - \epsilon'\right|} \left(2 \left(-\frac{1}{2a} \right) - \epsilon' \sqrt{a} + \frac{2}{a} \right) \\ &= \frac{2\pi}{\left|\frac{1}{\sqrt{a^3}} - \epsilon'\right|} \left(\frac{1}{a} - \epsilon' \sqrt{a} \right)\end{aligned}\tag{23}$$

The exceptional case, where the period (22) is undefined, is when $n = 1$, i. e. $a = 1$ and $\epsilon' = +1$. In this case solutions are stationary in rotating coordinates and lie on the unit circle with the free parameter ϕ_0 .

In general, the action of first kind generating orbits is positive if $\epsilon' = -1$, i. e. for all retrograde circular orbits I_r . Direct orbits exist for energies $H_0 = -1/(2a) - \epsilon' \sqrt{a} < -3/2$ and have negative action for radii $a > 1$ —direct exterior circular orbits I_{de} —and positive action for $a < 1$ —direct interior circular orbits I_{di} —with the action converging towards -2π and $+2\pi$ at the singularity, respectively. These orbits of negative action are not that interesting for us, because they only exist in the unbounded component of the Hill's region for energies below the first critical energy.

4.1.2 Second kind

First species orbits of the second kind are defined by mutually prime numbers of revolution I of M_2 and J of M_3 around M_1 in fixed coordinates. By Kepler's third law (4) the period is

$$\tau = 2\pi I = JT = 2\pi \sqrt{a^3} J,$$

and, hence, the semi-major axis a can be expressed as

$$a = \sqrt[3]{\frac{I^2}{J^2}}.$$

By the frequency (10) of the regularised ellipse, we know that the period of a full Kepler orbit in Levi-Civita regularised time is $S := s(T) = \pi/\varpi = \pi/\sqrt{-8H_{\text{fix}}}$. The action from (20) then becomes

$$\begin{aligned}\mathcal{A} &= JT(2H_{\text{fix}} + L) + 8JS \\ &= 2\pi \sqrt{a^3} J \left(2 \left(-\frac{1}{2a} \right) - \epsilon' \sqrt{a(1 - \epsilon^2)} \right) + \frac{8\pi J}{\sqrt{-8 \left(-\frac{1}{2a} \right)}} \\ &= 2\pi J \left(\sqrt{a} - \epsilon' a^2 \sqrt{1 - \epsilon^2} \right) \\ &= 2\pi \left(\sqrt[3]{IJ^2} - \epsilon' \sqrt[3]{\frac{I^4}{J}} \sqrt{1 - \epsilon^2} \right)\end{aligned}\tag{24}$$

and we see that while there are many combinations of I , J and ϵ that produce negative action, line (24) shows that the semi-major axis a must be greater than 1 on order for the action to become negative. So, in the bounded component \mathfrak{H}_c^b of the Hill's region no generating orbit of the first species can produce negative action.

4.2 Second species

A periodic second species generating orbit is a periodic sequence of Keplerian arcs joined at collision with M_2 . So in order to compute its action we need to compute the action of these arcs and add them up. Keplerian arcs are divided into four types as in section 3.2: Type 1 intersects the unit circle in two distinct points, type 2 is tangent to the unit circle at one point and types 3 and 4 are identical to the unit circle in retrograde and direct direction, respectively. Type 1 is subdivided into S-arcs and T-arcs, where in S-arcs the collisions occur in two distinct points on the unit circle, while T-arcs begin and end in collision on the same point on the unit circle in fixed coordinates. T-arcs can be computed as in the last section, since both M_2 and M_3 revolve an integer number of times during one arc. The same holds for arcs of type 2.

For S-arcs we shift time and rotate, such that at $t = 0$ the orbit is at its apocentre or pericentre and on the positive abscissa. We are going to compute the first intersection time of the regularised orbit with the unit circle in order to find the regularised period of the generating orbit. Setting the apocentre on the positive abscissa here corresponds to outgoing S-arcs, while the pericentre yields ingoing S-arcs. Remember that type 1 arcs require the pericentre to be closer than 1 and the apocentre to be farther away than 1 in order to get two distinct intersection points of the Kepler ellipse with the unit circle. The parametrisation of the regularised orbit can then be given from (11), (12) and (13) by

$$X_1(s) = \alpha \cos(\varpi s) \quad \text{and} \quad X_2(s) = \beta \sin(\varpi s),$$

where $\alpha = \sqrt{Q_1(0)}$ and $\beta = 2\dot{Q}_2(0)\sqrt{Q_1(0)}/\varpi$. The regularised orbit first intersects the unit circle at time $\sigma_0/2 > 0$ when

$$1 = X_1\left(\frac{\sigma_0}{2}\right)^2 + X_2\left(\frac{\sigma_0}{2}\right)^2.$$

Note that σ_0 is not necessarily the actual regularised period σ , since an S-arc can first wind around M_1 at the origin J times before colliding with M_2 again. The actual regularised period will then be $\sigma = JS + \sigma_0$. Obviously, the Levi-Civita transformation (8) preserves the unit circle, so an intersection with the unit circle in regularised coordinates corresponds to an intersection in usual coordinates. Inserting the parametrisation in

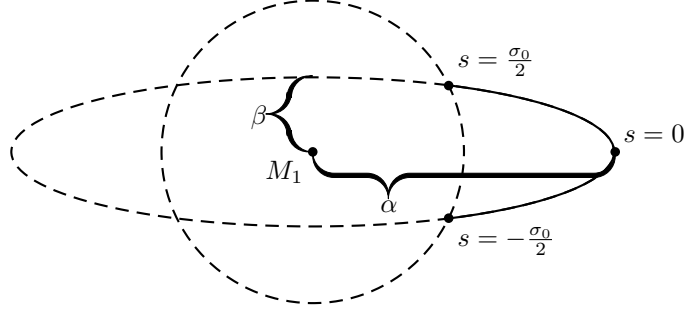


Figure 4: First intersection time of Levi-Civita-regularised Kepler ellipses with the unit circle.

regularised coordinates, one gets

$$\begin{aligned}
1 &= \alpha^2 \cos^2 \left(\varpi \frac{\sigma_0}{2} \right) + \beta^2 \sin^2 \left(\varpi \frac{\sigma_0}{2} \right) \\
&= \alpha^2 \cos^2 \left(\varpi \frac{\sigma_0}{2} \right) + \beta^2 \sin^2 \left(\varpi \frac{\sigma_0}{2} \right) + \beta^2 \cos^2 \left(\varpi \frac{\sigma_0}{2} \right) - \beta^2 \cos^2 \left(\varpi \frac{\sigma_0}{2} \right) \\
&= \beta^2 + \cos^2 \left(\varpi \frac{\sigma_0}{2} \right) (\alpha^2 - \beta^2) \\
\iff \cos^2 \left(\varpi \frac{\sigma_0}{2} \right) &= \frac{1 - \beta^2}{\alpha^2 - \beta^2} \\
\iff \sigma_0 &= \frac{2}{\varpi} \arccos \left(\sqrt{\frac{1 - \beta^2}{\alpha^2 - \beta^2}} \right).
\end{aligned}$$

Equivalences hold because $\varpi \sigma_0/2 \in (0, \pi)$ and $\beta^2 = \alpha^2 \iff \alpha = 1 \wedge \beta = \pm 1$. Both these latter cases do not admit an S-arc, but are rather of types 3 and 4, respectively. Using the formulae (10) for the angular frequency, (12) for α , and (13) for β in terms of the Kepler ellipse data, we get

$$\begin{aligned}
\sigma_0 &= \frac{2}{\sqrt{-8H_{\text{fix}}}} \arccos \left(\sqrt{\frac{1 - \beta^2}{\alpha^2 - \beta^2}} \right) \\
&= \frac{2}{\sqrt{-8 \left(-\frac{1}{2a}\right)}} \arccos \left(\sqrt{\frac{1 - a(1 - \epsilon)}{a(1 + \epsilon) - a(1 - \epsilon)}} \right) \\
&= \sqrt{a} \arccos \left(\sqrt{\frac{1 - a(1 - \epsilon)}{2a\epsilon}} \right). \tag{25}
\end{aligned}$$

Inserting this into the formula (20) for the action, we get

$$\begin{aligned}
\mathcal{A} &= (JT + \tau_0)(2H + L) + 8(JS + \sigma_0) \\
&= (2\pi\sqrt{a}J + \tau_0) \left(2 \left(-\frac{1}{2a} \right) - \epsilon' \sqrt{a(1 - \epsilon^2)} \right) + 8 \left(J \frac{\pi}{\varpi} + \sqrt{a} \arccos \left(\sqrt{\frac{1 - a(1 - \epsilon)}{2a\epsilon}} \right) \right) \\
&= (2\pi\sqrt{a}J + \tau_0) \left(-\frac{1}{a} - \epsilon' \sqrt{a(1 - \epsilon^2)} \right) + 8\sqrt{a} \left(\frac{\pi J}{2} + \arccos \left(\sqrt{\frac{1 - a(1 - \epsilon)}{2a\epsilon}} \right) \right),
\end{aligned} \tag{26}$$

where $\tau_0 = t(\sigma_0)$ is two times the first intersection time with the unit circle in normal time. This quantity has to be computed separately, which is done in the subsequent section.

The action of type 2 arcs is identical to the previous case of first species generating orbits of the second kind, since they are complete integer revolutions of Keplerian ellipses. Type 3 is half a circular retrograde Kepler orbit with radius $a = 1$ and identical with the circular retrograde generating orbit of family I_r with radius 1 and action $\mathcal{A} = 2\pi$. Type 4 on the other hand is in rotating coordinates the constant solution identical with M_2 at all times and therefore a third species generating orbit, which can not be computed using the Kepler problem.

4.3 Lambert's Theorem

A great tool that especially enables us to compute the elapsed time of Keplerian arcs of the second species is Lambert's theorem from [Lam61]. Its history, modern proofs and many remarks about it can be found in [Alb19] and [AU20]. We will state the main theorems and definitions needed for this work, while adapting the notation slightly. Objects of study for Lambert's theorem are Keplerian arcs beginning in point A at time t_A and ending in point B at time t_B in fixed coordinates.

Theorem 4.1 (Lambert, Theorem 1 in [Alb19]):

Consider Keplerian arcs around the origin O of \mathbb{R}^d . If we change continuously such an arc while keeping constant the distance $\|B - A\|$ between both ends, the sum of the radii $\|A\| + \|B\|$ and the energy H_{fix} , then the elapsed time $\tau_0 = t_B - t_A$ is also constant.

Theorem 4.2 (Lambert, Theorem 2 in [Alb19]):

Starting from any given Keplerian arc, we can arrive at some rectilinear arc by a continuous change which keeps constant the three quantities $\|B - A\|$, $\|A\| + \|B\|$ and H_{fix} .

Definition 4.3 (see Definition 5 in [Alb19]):

A Keplerian arc around O is called *simple* if its elapsed time is less than or equal to the period of its supporting ellipse. It is said to be *indirect*, or I_O , if its convex hull contains O ; *direct*, or D_O , if its convex hull does not contain O ; *indirect with respect to the second focus F* , or I_F , if its convex hull contains F ; *direct with respect to F* , or D_F , if its convex hull does not contain F .

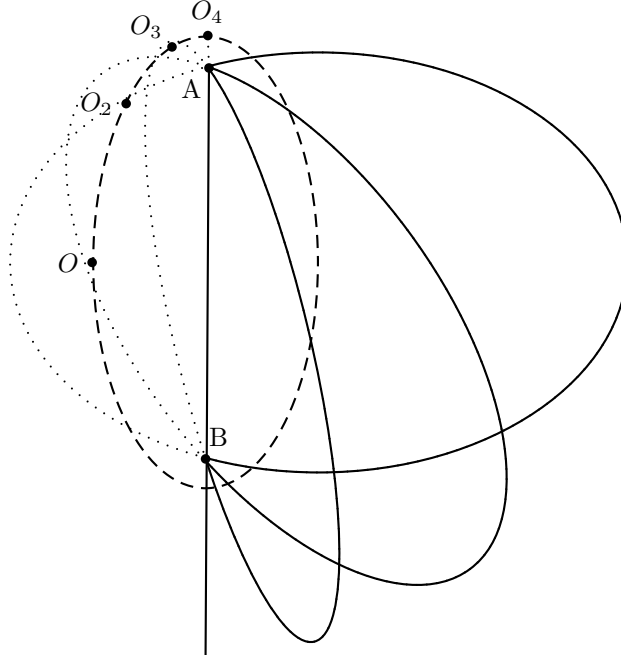


Figure 5: Lambert cycle of Keplerian arcs where the origin moves along a second ellipse with foci A and B .

In order to avoid confusion between terminologies we will only use the notation of I_O , D_O , I_F and D_F . The important feature of these types is that they are preserved during the *Lambert cycle*, which is the continuous change of Keplerian arcs as in theorem 4.1:

Proposition 4.4 (Proposition 5 in [Alb19]):

If a Keplerian arc in a Lambert cycle is I_O or D_O and I_F or D_F , then all the Keplerian arcs of the cycle are I_O or D_O and I_F or D_F , respectively.

In our case of second species generating orbits we have as parameters the semi-major axis a , the eccentricity ϵ and the polar angle θ of the intersection with the unit circle. They are interrelated by the equation for the polar distance

$$r(\theta) = \frac{a(1 - \epsilon^2)}{1 - \epsilon \cos \theta} \quad (27)$$

of an ellipse with one focus in the origin, so we have

$$\cos \theta = \frac{1 - a(1 - \epsilon^2)}{\epsilon}.$$

The elapsed time can then be computed with the help of theorem 4.1 and 4.2 by the elapsed time of a rectilinear arc. Since the energy $H_{\text{fix}} = -1/(2a)$ remains constant, the semi-major axis remains constant during the continuous change and, consequently, the supporting rectilinear orbit has length $2a$. We can follow the shape of the supporting ellipse during the continuous change by shifting the focus of the ellipse along a second ellipse with foci A and B going through the origin. The semi-major axis of this second ellipse is 1 in our case, since A and B lie on the unit circle, and therefore the elapsed time can be computed by using the free-fall time (14) from height $2a$ to A and to B .

By Proposition 4.4, depending on whether the original arc was I_O or D_O and I_F or D_F , the new rectilinear arc will also be I_O or D_O and I_F or D_F , respectively. The original arc is

$$\left\{ \begin{array}{l} I_O \quad \text{if } \theta \geq \frac{\pi}{2} \\ D_O \quad \text{if } \theta < \frac{\pi}{2} \end{array} \right\} \quad \text{and} \quad \left\{ \begin{array}{l} I_F \quad \text{if } 2a\epsilon \geq \cos \theta \\ D_F \quad \text{if } 2a\epsilon < \cos \theta \end{array} \right\},$$

and we can state the following conclusion:

Lemma 4.5:

The elapsed time of an outgoing second species generating arc is

$$\tau = 2\pi J\sqrt{a^3} + \begin{cases} t_{2a}(1 + \sin \theta) + t_{2a}(0) + (t_{2a}(0) - t_{2a}(1 - \sin \theta)) & \text{if } \cos \theta \leq 0 \\ t_{2a}(1 + \sin \theta) + t_{2a}(1 - \sin \theta) & \text{if } 0 < \cos \theta \leq 2a\epsilon \\ t_{2a}(1 + \sin \theta) - t_{2a}(1 - \sin \theta) & \text{if } 2a\epsilon < \cos \theta. \end{cases}$$

Remark 4.6:

There is no case I_O and D_F . If we rotate the arc such that the apoapsis—which has to be farther away than 1—lies on the Q_1 -axis, then the second focus lies between the apoapsis and the origin on the Q_1 -axis. Hence, if an outgoing arc is I_O , it is necessarily also I_F . The times of ingoing second species arcs are simply $2\pi\sqrt{a^3} = 2t_{2a}(0)$ minus the outgoing time.

The orbits which we will construct in the next section will only be outgoing second species generating orbits without M_3 winding around M_1 , i. e. with $J = 0$. This restriction makes sense particularly in view of (19), where for negative angular momentum the only positive contribution to the action comes from the term $1/\|Q\|$ which we try to keep as small as possible in order to get negative action. In this situation the following statement helps us to exclude orbits without winding of M_2 around M_1 .

Theorem 4.7 (Theorem 7.2 from [AU20]):

In the Euclidean plane or space consider three distinct points O, A, B such that O is not on the segment AB . There is a unique D_O Keplerian arc around O and a unique simple I_O Keplerian arc around O going from A to B in a given positive elapsed time. In the exceptional case $O \in]A, B[$ there exist exactly two distinct I_O Keplerian arcs which are reflections of each-other.

Corollary 4.8:

There exist no S-arcs with $I = J = 0$ and $\epsilon' = +1$ which are not identical to M_2 at all times.

Proof: An S-arc requires a Keplerian arc with two distinct ends A and B on the unit circle. The timing condition for $I = J = 0$ requires that the elapsed time of the arc is exactly the elapsed time of M_2 between A and B . Since both M_2 and M_3 move in the same direct direction around M_1 , the arc of M_3 is D_O and I_O if and only if the arc of M_2 is D_O and I_O , respectively. Uniqueness in theorem 4.7 give us that both arcs are the same and hence M_3 coincides with M_2 for all time. \square

4.4 Sequences of generating orbits

We will now describe some sequences of generating orbits and also show where they are found in terms of Hénon's notation for generating families. Using our formulae from the previous sections of this chapter, we can find generating orbits with negative action that have additional properties. In our case we want to control the energy and show that these orbits exist for all energies between $-\sqrt{2}$ and 0. All generating orbits described here will be of the second species, but not all orbits in this section will actually have negative action. They are then rather included here either because they are instructive and arise in Hénon's classification of families or because they are at the beginning of a sequence where the action tends towards negative values but is not necessarily negative throughout the entire sequence.

The main formula we will use to compute the action is equation (26), which is quite powerful but still requires the elapsed time of the Kepler arc between collisions with M_2 . Since the Kepler arc corresponding to the generating orbit is usually not a full Kepler ellipse, we will use Lemma 4.5 for the remaining cases. To further simplify things, we will always set $J = 0$, i. e. the arc of M_3 does not wind around M_1 in fixed coordinates. The reason for this is equation (19), where the only term contributing positively to the action is $1/\|Q\|$ and we intend to keep this term small by not letting the orbit come unnecessarily close to M_1 . Also, our generating orbits here will only consist of a single outgoing S -arc which is repeated infinitely to give a periodic generating orbit.

Another issue in order to analytically describe second species generating orbits is the timing condition

$$\tau = \begin{cases} 2\pi I + 2\theta & \text{for direct and rectilinear orbits} \\ 2\pi(I + 1) - 2\theta & \text{for retrograde orbits,} \end{cases} \quad (28)$$

i. e. the requirement that M_3 collides again with M_2 after starting at collision and following the arc. This problem is avoided in this chapter by leaving a free parameter which will be the semi-major axis a of the supporting Kepler ellipse. We will then show that $\tau - 2\epsilon'\theta$ tends smoothly towards infinity as $a \rightarrow \infty$. This means that for all large enough numbers of revolution I of M_2 around M_1 in fixed coordinates there will be an a that solves the timing condition for that particular I . A one-parameter family with a as

the free parameter will in this way give a sequence of second species generating orbits with an orbit for each large enough integer $I \geq 1$. Other parameters of the supporting Keplerian orbit which will be used in this section are the eccentricity ϵ , the semi-minor axis b , the polar angle of intersection with the unit circle θ and the direction of rotation ϵ' .

4.4.1 Fixed semi-minor axis

The first sequence we want to present is one where the energy converges towards zero and the action against negative infinity. This can be achieved by fixing the semi-minor axis b . The relation between b , a and ϵ is $b = a\sqrt{1 - \epsilon^2}$, i. e.

$$\epsilon = \sqrt{1 - \frac{b^2}{a^2}}. \quad (29)$$

Inserting this into the Kepler energy (5) and the angular momentum (6), the rotating Kepler energy (2) becomes

$$H_0 = -\frac{1}{2a} - \epsilon' \frac{b}{\sqrt{a}} \quad (30)$$

which strictly monotonically tends towards zero from below as $a \rightarrow \infty$ and $\epsilon' = +1$ for any fixed b . We choose the easiest nonzero $b = 1$ for the sequence.

In order to define an outgoing arc not part of the unit circle, we need the maximal focal distance

$$a(1 + \epsilon) = a + \sqrt{a^2 - 1} > 1, \quad \text{i. e.} \quad a > 1.$$

For the elapsed time of the arc we use Lemma 4.5, for which we need $\sin \theta$. Also, we need to check if the arcs are I_O and I_F , or D_O and I_F , or D_O and D_F . We can compute $\cos \theta$ from the equation for focal distances of ellipses (27):

$$\cos \theta = \frac{1 - a(1 - \epsilon^2)}{\epsilon} = \frac{1 - \frac{1}{a}}{\sqrt{1 - \frac{1}{a^2}}} = \sqrt{\frac{a-1}{a+1}}$$

Since $a > 1$, we have

$$0 < \cos \theta = \sqrt{\frac{a-1}{a+1}} < 2\sqrt{(a-1)(a+1)} = 2a\epsilon,$$

i. e. all arcs in this sequence are D_O and I_F , and we can compute

$$\begin{aligned}
\tau &= t_{2a}(1 - \sin \theta) + t_{2a}(1 + \sin \theta) \\
&= 2\sqrt{a^3} \left(\sqrt{\frac{1 - \sin \theta}{2a} \left(1 - \frac{1 - \sin \theta}{2a}\right)} + \sqrt{\frac{1 + \sin \theta}{2a} \left(1 - \frac{1 + \sin \theta}{2a}\right)} \right. \\
&\quad \left. + \arccos \left(\sqrt{\frac{1 - \sin \theta}{2a}} \right) + \arccos \left(\sqrt{\frac{1 + \sin \theta}{2a}} \right) \right), \tag{31}
\end{aligned}$$

where

$$\sin \theta = \sqrt{1 - \cos^2 \theta} = \sqrt{1 - \frac{a-1}{a+1}} = \sqrt{\frac{2}{a+1}}. \tag{32}$$

Obviously, the elapsed time tends towards infinity as $a \rightarrow \infty$. In particular for $\epsilon' = +1$ the time $\tau - 2\theta$ becomes zero for the limit case $a = 1$ and depends smoothly on a . So there exists for every $I \geq 1$ an $a > 1$ solving the timing condition (28) and we get a sequence of second species generating orbits.

The regularised time from (25) becomes

$$\begin{aligned}
\sigma &= \sqrt{a} \arccos \left(\sqrt{\frac{1 - a(1 - \epsilon)}{2a\epsilon}} \right) \\
&= \sqrt{a} \arccos \left(\sqrt{\frac{1 - a \left(1 - \sqrt{1 - \frac{1}{a^2}}\right)}{2\sqrt{a^2 - 1}}} \right) \\
&= \sqrt{a} \arccos \left(\sqrt{\frac{1}{2} - \frac{1}{2}\sqrt{\frac{a-1}{a+1}}} \right) \tag{33}
\end{aligned}$$

and by inserting (29), (31) and (33) into (20), we get the action of these generating orbits:

$$\begin{aligned}
\mathcal{A} &= 2\sqrt{a^3} \left(-\frac{1}{a} - \epsilon' \frac{1}{\sqrt{a}} \right) \left(\sqrt{\frac{1 - \sqrt{\frac{2}{a+1}}}{2a} \left(1 - \frac{1 - \sqrt{\frac{2}{a+1}}}{2a}\right)} \right. \\
&\quad \left. + \sqrt{\frac{1 + \sqrt{\frac{2}{a+1}}}{2a} \left(1 - \frac{1 + \sqrt{\frac{2}{a+1}}}{2a}\right)} + \arccos \left(\sqrt{\frac{1 - \sqrt{\frac{2}{a+1}}}{2a}} \right) + \arccos \left(\sqrt{\frac{1 + \sqrt{\frac{2}{a+1}}}{2a}} \right) \right) \\
&\quad + 8\sqrt{a} \arccos \left(\sqrt{\frac{1}{2} - \frac{1}{2}\sqrt{\frac{a-1}{a+1}}} \right)
\end{aligned}$$

This tends towards negative infinity as a goes towards infinity.

Summarising so far, we can state

Lemma 4.9:

There exists a sequence of second species generating orbits consisting of non-rectilinear S -arcs with semi-major axis $a > 1$, action tending towards negative infinity and energy H_0 strictly monotonically converging towards zero from below.

4.4.2 Fixed polar intersection angle with the unit circle

For more general sequences we fix the angle of intersection θ with the unit circle. We will look at all $\theta \in [0, \pi]$ but we will also highlight some special cases that arise. Let from now on $a > 1$. The eccentricity is computed by solving the equation (27) of the focal distance of ellipses for ϵ :

$$1 = \frac{a(1 - \epsilon^2)}{1 - \epsilon \cos \theta}$$

$$\iff a\epsilon^2 - \epsilon \cos \theta - a + 1 = 0$$

$$\iff \epsilon = \frac{\cos \theta \pm \sqrt{\cos^2 \theta + 4a(a - 1)}}{2a} \tag{34}$$

$$\stackrel{\epsilon \geq 0}{\iff} \epsilon = \frac{\cos \theta + \sqrt{\cos^2 \theta + 4a(a - 1)}}{2a} \tag{35}$$

Remark 4.10:

There exist ellipses intersecting the unit circle at polar angle $\theta \in [0, \pi/2]$ also for semi-major axes $a \leq 1$. However, a is no longer a monotone parameter there. Now both signs of (34) return nonnegative eccentricity. The actually smallest semi-major axis is attained at the largest root of the discriminant $\cos^2 \theta + 4a(a - 1)$. A better parameter for small a would for example be the eccentricity ϵ —see also proposition 2.5 in [AU20]—but we will stick to the semi-major axis as our parameter because computations of the energy and action are easier. Another advantage of setting $a > 1$ is that

$$2a\epsilon = \cos \theta + \sqrt{\cos^2 \theta + 4a(a - 1)} > \cos \theta, \tag{36}$$

i. e. all arcs are I_F .

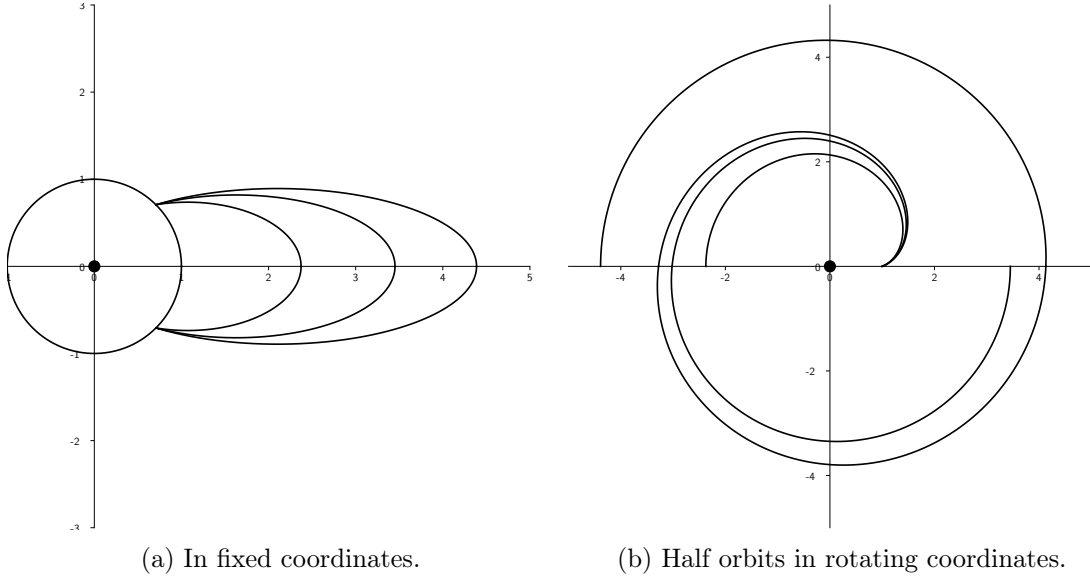


Figure 6: Second species arcs with fixed $\theta = \pi/4$ and $I = 1, 2$.

The energy becomes

$$\begin{aligned}
H_0 &= -\frac{1}{2a} - \epsilon' \sqrt{a(1 - \epsilon^2)} \\
&= -\frac{1}{2a} - \epsilon' \sqrt{a \left(1 - \frac{(\cos \theta + \sqrt{\cos^2 \theta + 4a(a-1)})^2}{4a^2} \right)} \\
&= -\frac{1}{2a} - \epsilon' \sqrt{\frac{4a^2 - \cos^2 \theta - 2 \cos \theta \sqrt{\cos^2 \theta + 4a(a-1)} - \cos^2 \theta - 4a(a-1)}{4a}} \\
&= -\frac{1}{2a} - \epsilon' \sqrt{1 - \cos \theta \frac{\cos \theta + \sqrt{4a^2 - 4a + \cos^2 \theta}}{2a}} \xrightarrow{a \rightarrow \infty} -\epsilon' \sqrt{1 - \cos \theta} \quad (37)
\end{aligned}$$

and tends towards values between $-\sqrt{2}$ and $\sqrt{2}$ depending on θ and ϵ' . It was also computed in lemma 3.8 that the derivative $\partial H_0 / \partial a$ never vanishes, so the energy strictly increases for $\epsilon' = +1$ and strictly decreases for $\epsilon' = -1$ along a .

In the first case $\theta < \pi/2$ all arcs are D_O and I_F , and we compute the elapsed time

from lemma 4.5 to be

$$\begin{aligned}
\tau &= t_{2a}(1 + \sin \theta) + t_{2a}(1 - \sin \theta) \\
&= 2\sqrt{a^3} \left(\sqrt{\frac{1 - \sin \theta}{2a} \left(1 - \frac{1 - \sin \theta}{2a}\right)} + \sqrt{\frac{1 + \sin \theta}{2a} \left(1 - \frac{1 + \sin \theta}{2a}\right)} \right. \\
&\quad \left. + \arccos \left(\sqrt{\frac{1 - \sin \theta}{2a}} \right) + \arccos \left(\sqrt{\frac{1 + \sin \theta}{2a}} \right) \right). \tag{38}
\end{aligned}$$

In the second case $\theta \geq \pi/2$ all arcs are I_O and I_F , and we use the first case in lemma 4.5, so

$$\begin{aligned}
\tau &= t_{2a}(1 + \sin \theta) + t_{2a}(0) + (t_{2a}(0) - t_{2a}(1 - \sin \theta)) \\
&= 2\sqrt{a^3} \left(\sqrt{\frac{1 + \sin \theta}{2a} \left(1 - \frac{1 + \sin \theta}{2a}\right)} + \arccos \left(\sqrt{\frac{1 + \sin \theta}{2a}} \right) + \frac{\pi}{2} \right. \\
&\quad \left. + \left(\frac{\pi}{2} - \sqrt{\frac{1 - \sin \theta}{2a} \left(1 - \frac{1 - \sin \theta}{2a}\right)} - \arccos \left(\sqrt{\frac{1 - \sin \theta}{2a}} \right) \right) \right).
\end{aligned}$$

It is obvious in both cases that for fixed θ the elapsed time τ increases strictly and tends towards infinity as $a \rightarrow \infty$ because τ is only the sum of free-fall times to the same points from increased heights $2a$. This means the timing condition (28) has a unique solution for every large enough $I \geq 1$. Note that corollary 4.8 states that there is no nontrivial solution for $I = 0$. We also see that the assumption $a > 1$ is no restriction, since for $a = 1$ and $\theta > 0$ we get

$$\tau < 2t_2(0) = 2\pi < 2\pi + 2\theta.$$

Hence, the timing condition for $\epsilon' = +1$, $I = 1$ and any fixed $\theta > 0$, is always satisfied for an $a > 1$. The case $\theta = 0$ will later be treated separately.

The regularised time is

$$\begin{aligned}
\sigma &= \sqrt{a} \arccos \left(\sqrt{\frac{1 - a(1 - \epsilon)}{2a\epsilon}} \right) \\
&= \sqrt{a} \arccos \left(\sqrt{\frac{\frac{2 - 2a + \cos \theta + \sqrt{\cos^2 \theta + 4a(a - 1)}}{2}}{\cos \theta + \sqrt{\cos^2 \theta + 4a(a - 1)}}} \right) \\
&= \sqrt{a} \arccos \left(\sqrt{\frac{1}{2} - \frac{a - 1}{\cos \theta + \sqrt{\cos^2 \theta + 4a(a - 1)}}} \right)
\end{aligned}$$

and the action from (26) becomes

$$\begin{aligned} \mathcal{A} = & \tau \left(-\frac{1}{a} - \epsilon' \sqrt{1 - \cos \theta} \frac{\cos \theta + \sqrt{4a^2 - 4a + \cos^2 \theta}}{2a} \right) \\ & + 8\sqrt{a} \arccos \left(\sqrt{\frac{1}{2} - \frac{a-1}{\cos \theta + \sqrt{\cos^2 \theta + 4a(a-1)}}}} \right). \end{aligned} \quad (39)$$

The important feature is that the action tends towards negative infinity for every fixed and positive θ as $a \rightarrow \infty$ and $\epsilon' = +1$ since the angular momentum tends towards $\sqrt{1 - \cos \theta}$. This holds in both cases $\theta < \pi/2$ and $\theta \geq \pi/2$ since $\sqrt{a^3}$ multiplied by bounded terms outweighs the only positive term of \sqrt{a} times something bounded.

In the limit case $\theta = 0$, however, the angular momentum vanishes completely and we get

$$\begin{aligned} H_0 &= -\frac{1}{2a} \\ \tau &= 2\sqrt{a^3} \left(2\sqrt{\frac{1}{2a} \left(1 - \frac{1}{2a} \right)} + 2 \arccos \left(\sqrt{\frac{1}{2a}} \right) \right) \\ \sigma &= \sqrt{a} \arccos \left(\sqrt{\frac{1}{2a}} \right) \end{aligned}$$

and hence

$$\begin{aligned} \mathcal{A} &= -\frac{4}{a} \sqrt{a^3} \left(\sqrt{\frac{1}{2a} \left(1 - \frac{1}{2a} \right)} + \arccos \left(\sqrt{\frac{1}{2a}} \right) \right) + 8\sqrt{a} \arccos \left(\sqrt{\frac{1}{2a}} \right) \\ &= 4\sqrt{a} \arccos \left(\sqrt{\frac{1}{2a}} \right) - 2\sqrt{2 - \frac{1}{a}}. \end{aligned}$$

The action here no longer tends towards negative values and is in fact always nonnegative. In fixed coordinates M_3 would fall freely towards M_1 —where we would have to regularise—and then bounce back to the place it started. In our setting of an outgoing generating orbit of the second species with $J = 0$, however, M_3 would not make it that far since it would first collide with M_2 moving on the unit circle.

Two more special cases will be mentioned here: the case $\theta = \pi/2$ and $\theta = \pi$. For $\theta = \pi$

the arcs are full Kepler ellipses, i. e. second species of type 2. We get

$$\begin{aligned} H &= -\frac{1}{2a} - \epsilon' \sqrt{2 - \frac{1}{a}} \\ \tau &= 2\pi\sqrt{a^3} \\ \sigma &= \frac{\pi\sqrt{a}}{2} \end{aligned}$$

and

$$\begin{aligned} \mathcal{A} &= 2\pi\sqrt{a^3} \left(-\frac{1}{a} - \epsilon' \sqrt{2 - \frac{1}{a}} \right) + 8\frac{\pi\sqrt{a}}{2} \\ &= 2\pi\sqrt{a} - 2\pi\epsilon'a\sqrt{2a-1}. \end{aligned}$$

This action obviously has the same sign as $-\epsilon'$ for all $a > 1$. Since these generating orbits are both first and second species orbits, they are naturally bifurcation orbits. In the continuation to the restricted three-body problem the intersection of the corresponding families splits into two separate families here.

In the remaining special case we fix $\theta = \pi/2$. The data simplifies to

$$\begin{aligned} H_0 &= -\frac{1}{2a} - \epsilon', \\ \tau &= 2\sqrt{a^3} \left(\sqrt{\frac{1}{a} \left(1 - \frac{1}{a} \right)} + \arccos \left(\sqrt{\frac{1}{a}} \right) + \frac{\pi}{2} \right) \\ &= \pi\sqrt{a^3} + 2\sqrt{a(a-1)} + 2\sqrt{a^3} \arccos \left(\sqrt{\frac{1}{a}} \right), \\ \sigma &= \sqrt{a} \arccos \left(\sqrt{\frac{1}{2} - \frac{a-1}{\sqrt{4a(a-1)}}} \right) \\ &= \sqrt{a} \arccos \left(\sqrt{\frac{1}{2} - \frac{1}{2}\sqrt{\frac{a-1}{a}}} \right) \end{aligned}$$

and

$$\begin{aligned} \mathcal{A} &= \left(\pi\sqrt{a^3} + 2\sqrt{a(a-1)} + 2\sqrt{a^3} \arccos \left(\sqrt{\frac{1}{a}} \right) \right) \left(-\frac{1}{a} - \epsilon' \right) \\ &\quad + 8\sqrt{a} \arccos \left(\sqrt{\frac{1}{2} - \frac{1}{2}\sqrt{\frac{a-1}{a}}} \right). \end{aligned}$$

What happens here is that in fixed coordinates the angular velocity of M_3 exactly matches

that of M_2 at the point of collision:

$$\frac{d\varphi}{dt} = \frac{L}{r^2} = \sqrt{a(1-\epsilon^2)} = \sqrt{a\left(1 - \frac{4a(a-1)}{4a^2}\right)} = 1 \quad (40)$$

Theorem 3.6 can no longer exclude a collision in the perturbation to the restricted three-body problem because the ingoing and outgoing vectors in rotating coordinates are parallel. So, at this point a new loop forms around M_2 . More explicitly, in the restricted three-body problem, orbits coming from generating orbits with $\theta < \pi/2$ will wind $I - 1$ times around both M_1 and M_2 and then pass in between M_1 and M_2 , while orbits coming from generating orbits with $\theta > \pi/2$ will wind $I - 1$ times around M_1 and then wind once around M_2 before starting over. This transition from $\theta = \pi$ and $\epsilon' = -1$ to $\theta = \pi$ and $\epsilon' = +1$ via $\theta = 0$ happens in the $\{S_{-\alpha-1}\}$ segments in families f and h as described in [Hén97]. For generating orbits with $I = 1$ and corresponding continued orbits in the restricted three-body problem for small mass ratios as θ crosses $\pi/2$ see also figure 9 in the next chapter.

Generating family f —see figure 7a—comes from the simple direct orbits in Hill’s lunar problem and transitions into family $E_{1,1}^+$ of first species generating orbits at the critical point with energy $H_0 = -3/2$ and abscissa $q_1(0) = 1$ for negative $\dot{q}_2(0)$. It follows $E_{1,1}^+$ with growing energy, undergoes collision with M_1 at $H_0 = -1/2$ and $q_1(0) = 2$, and picks up a loop around M_1 there. The generating family arrives at $H_0 = 1/2$ and $q_1(0) = 1$ as a double cover of the retrograde circular orbit, which is also a second species orbit with $\theta = \pi$ and $\epsilon' = -1$. From there it follows the branch of second species generating orbits $S_{-2,-1}$, transitioning to $\theta = \pi$ and $\epsilon' = +1$ and picking up a loop at $\theta = \pi/2$ and $\epsilon' = +1$ as described above. The last orbit at $\theta = \pi$ is again a first species orbit in the family $E_{3_1}^+$ and this cycle continues indefinitely between $E_{2k-1,1}^+$ and $S_{-2k,-1}$ for all $k > 0$.

Family h comes from the retrograde circular orbits I_r and then at $a = 1$ goes into the branch $S_{-1,-1}$ at $\theta = \pi/2$ and $\epsilon' = -1$. Then it goes along, while taking up a loop, to $\theta = \pi$ and $\epsilon' = +1$ as described above. There, it takes the branch of first species family $E_{2,1}$, which takes up another loop at collision with M_1 , and carries on until the inner loop collides with M_2 again. From there on it resumes a similar pattern as family f and alternates between $S_{-2k-1,-1}$ and $E_{2k,1}$ for all $k > 0$.

The summary of the information from this chapter which is important for the proof of the main theorem is

Lemma 4.11:

For every $c \in [-\sqrt{2}, 0]$ there exists a sequence of second species generating orbits consisting of S -arcs with action tending towards negative infinity and energy converging strictly from below to c .

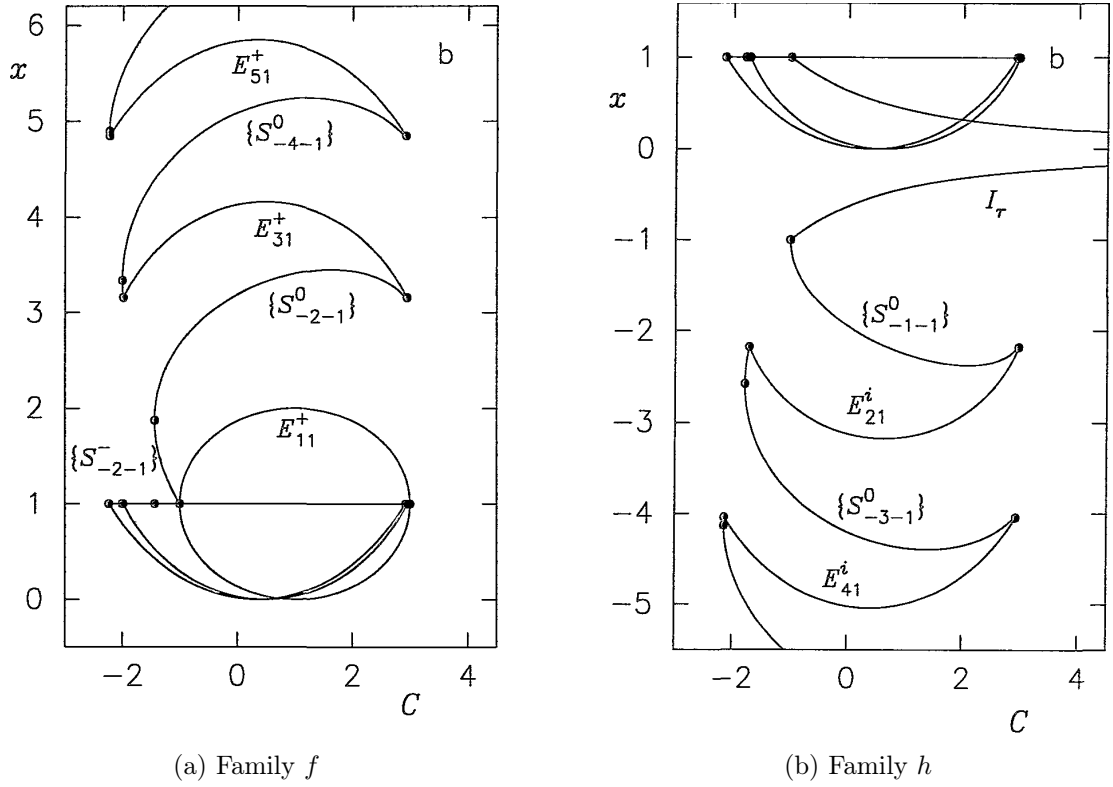


Figure 7: Two symmetric families of generating orbits as shown in [Hén97].

5 Proof of main theorem

We are now ready to put everything together and show up the consequences of these orbits for the existence of contact structures in the restricted three-body problem. For this we first of all want to improve lemma 4.11. In fact, we can get sequences of orbits with negative action tending towards negative infinity with constant energy at any value between $-\sqrt{2}$ and 0. We can also choose these sequences such that all orbits are ordinary and nondegenerate. This is particularly helpful since the statement of theorem 3.6 finds orbits close to the generating orbit with the exact same energy under these circumstances.

Lemma 5.1:

For every $c \in [-\sqrt{2}, 0)$ there exists a sequence of ordinary nondegenerate generating orbits of the second species with energy c and negative action tending to $-\infty$.

Proof: As we have seen in the preceding chapter 4, there exists for every polar intersection angle $\theta \in [0, \pi]$ with the unit circle and every number of rotation $I \geq 1$ a unique second species arc. For $\epsilon' = +1$ these arcs have energy converging strictly monotonically to $-\sqrt{1 - \cos\theta}$ from below and their action tends to $-\infty$ if $\theta > 0$ as $I \rightarrow \infty$. Since the elapsed time τ and the energy $H_0 = c$ of the arcs depend smoothly on θ , we get for

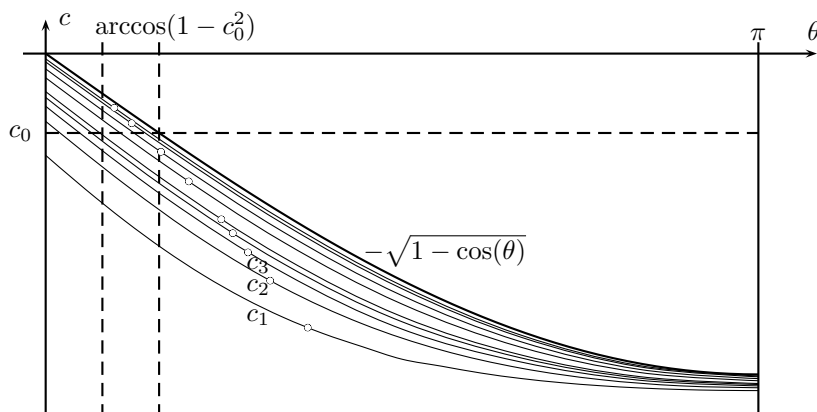


Figure 8: The curves c_I mapping a simple direct arc of polar intersection angle θ to its energy.

every $I \geq 1$ a smooth curve

$$c_I: [0, \pi] \rightarrow \mathbb{R}$$

mapping θ to the energy of the unique direct arc where the timing condition (28) is satisfied for I and θ . The sequences for all fixed θ are strictly increasing in c along a , so we have $c_{I_1} < c_{I_2}$ for all $I_1 < I_2$ and the curves c_I converge to $-\sqrt{1 - \cos \theta}$ as $I \rightarrow \infty$.

Let $c_0 \in [-\sqrt{2}, 0)$. We restrict the curves c_I to $[\arccos(1 - c_0^2)/2, \pi] \subset (0, \pi]$. Here, for all sequences of arcs with fixed θ , the action tends towards $-\infty$ as $a \rightarrow \infty$. So we can find for every $\theta \in [\arccos(1 - c_0^2)/2, \pi]$ an $N_\theta > 0$ such that the action of the arc with polar intersection angle θ and semi-major axis $a > N_\theta$ is negative. Assign this real number N_θ to every θ by the smooth function

$$N: [\arccos(1 - c_0^2)/2, \pi] \rightarrow \mathbb{R} \\ \theta \mapsto N_\theta.$$

Then N attains its maximum \hat{N} at some point and for all $\theta \in [\arccos(1 - c_0^2)/2, \pi]$ and $a > \hat{N}$ the corresponding arcs have negative action.

To find the smallest I where every point on the curve c_I is attained for an arc with semi-major axis $a > \hat{N}$, we look at solutions of the timing condition for all real $I_\theta \in (1, \infty)$. Again we assign this value to every arc with semi-major axis $a = \hat{N}$ and $\theta \in [\arccos(1 - c_0^2)/2, \pi]$ by the smooth function

$$I: [\arccos(1 - c_0^2)/2, \pi] \rightarrow (1, \infty) \subset \mathbb{R} \\ \theta \mapsto I_\theta.$$

This, again, attains its maximum $\hat{I} \in (0, \infty)$ at some point. So for all integers $I > \hat{I}$ we

have full curves $c_I: [\arccos(1 - c_0^2)/2, \pi] \rightarrow (-\infty, 0)$ corresponding to arcs with semi-major axis $a > \hat{N}$, i. e. with negative action. Finally,

$$\left\{ (\theta, c_I(\theta)) \mid I > \hat{I}, \theta \in [\arccos(1 - c_0^2)/2, \pi) \right\} \cap \left\{ (\theta, c_0) \mid \theta \in [\arccos(1 - c_0^2)/2, \pi) \right\}$$

is a sequence of points on the graphs $\bigcup_I \Gamma(c_I)$ converging to $(\arccos(1 - c_0^2), c_0)$. There are no degenerate or non-ordinary orbits in these sequences anymore since $\theta \neq 0, \pi$. Furthermore, the only orbits with parallel velocities at collision in these sequences are where the arcs intersect the unit circle with angle $\theta = \pi/2$. We can simply exclude these, since this affects at most one single element in the sequence. Hence, we have found a sequence of ordinary nondegenerate second species generating orbits with energy c_0 and negative action.

By doing the same process again for an arbitrarily small action we can show that the action of orbits in this sequence indeed tends towards $-\infty$. \square

In a next step we will check the integral of the first de Rham generator β_0 —which was computed in 2.1—along the continued orbits that we get from the sequences of generating orbits.

Lemma 5.2:

Let γ be an orbit in one of the sequences from lemma 5.1 and γ_μ a continuation to the restricted three-body problem with mass ratio μ by theorem 3.6. Then the integral over the first de Rham generator β_0 of $\bar{\Sigma} \cong \bar{\Sigma}_{\mu,c}$ along γ_μ is

$$\int_S^1 \gamma_\mu^* \beta_0 = -1.$$

Proof: As in the proof of 5.1, the initial and final velocities of the generating arc at collision are non-parallel in rotating coordinates and by theorem 3.6 the continued orbit γ_μ does not collide with M_2 . We can compute the integral over $\beta_0|_{\Sigma_{\mu,c}} = 2d\vartheta - d\varphi_1 - d\varphi_2$ by two times the rotation number minus the two winding numbers around M_1 and M_2 .

In the case $\theta \in (0, \pi/2)$ the angle between the initial and final velocities of the generating arc at collision is between 0 and π in rotating coordinates. The continuation uses hyperbolic solutions on the Levi-Civita regularisation close to M_2 and all arcs are outgoing. So the continued orbit passes between M_1 and M_2 on a trajectory that looks like a hyperbola close to M_2 . Recall the integer numbers of rotation I and J of M_2 and M_3 around M_1 . In all of our sequences we have $J = 0$ while $I \geq 1$. This gives us the rotation number $-I$, the winding number $-I$ around M_1 and the winding number $-I + 1$ around M_2 . Overall, this gives

$$\int_{S^1} \gamma_\mu^* \beta_0 = -2I + I + I - 1 = -1.$$

In the case $\theta \in (\pi/2, \pi)$ the angle between initial and final velocity at collision is in between π and 2π , and the angular velocity dropping below one—see(40)—forming an additional loop around M_2 in the continuation. Therefore, the rotation number

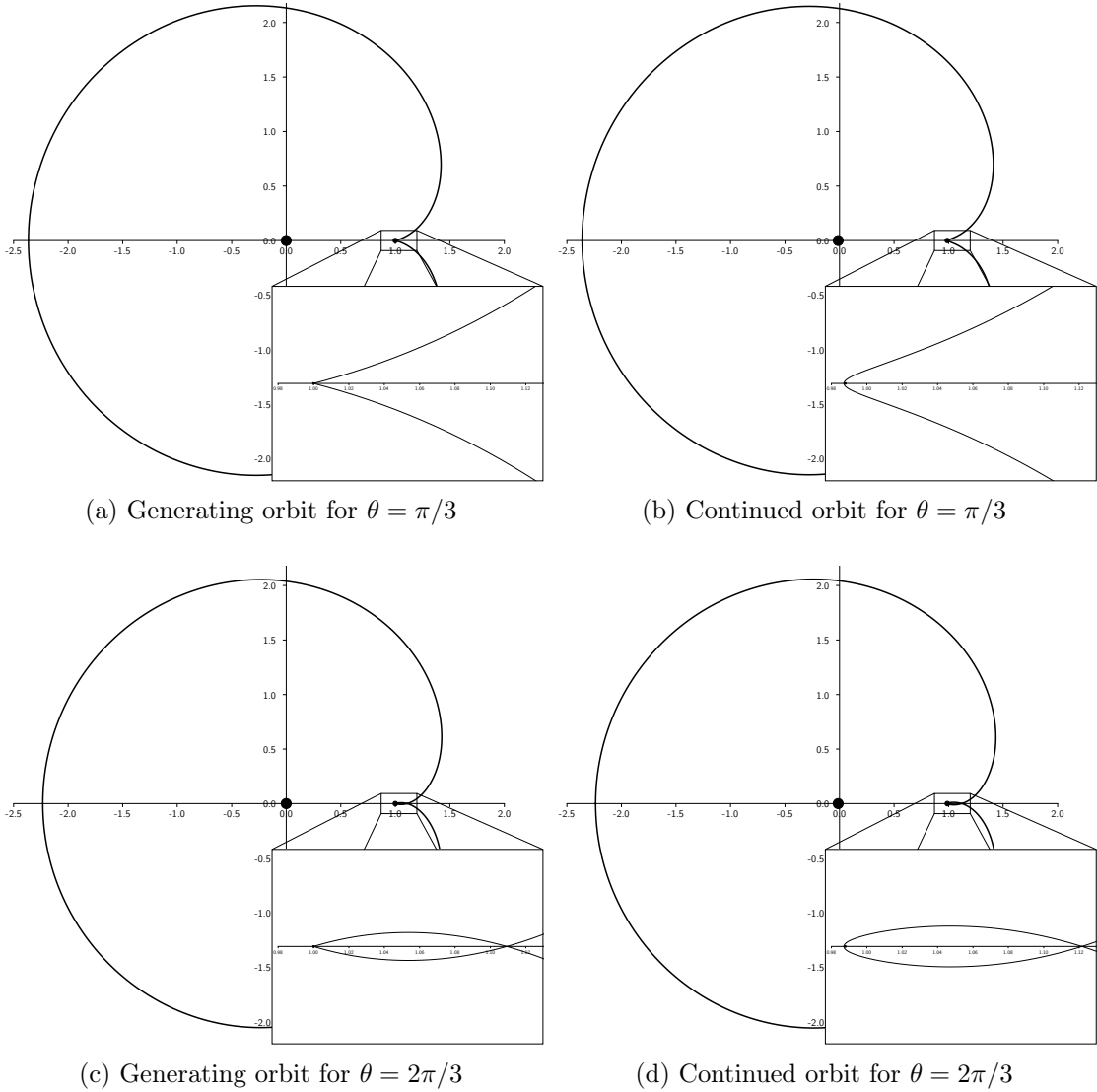


Figure 9: Generating orbits as θ crosses $\pi/2$ and their continuations at the same energy level in the restricted three-body problem with earth-moon mass ratio $\mu = 0.01214$.

becomes $-I - 1$, the winding numbers $-I$ around M_1 and $-I - 1$ around M_2 . All in all we get the same integral

$$\int_{S^1} \gamma_{\mu}^* \beta_0 = 2(-I - 1) + I + I + 1 = -1,$$

as claimed. \square

Before we can finally prove the main theorem, we first need to discuss exactly what

Hamiltonian structures and primitives we are dealing with:

Let $\bar{\Sigma}_{\mu,c}$ be the Moser-regularised energy hypersurface of the restricted three-body problem with mass ratio $\mu \in (0, 1)$ for an energy $c > H_\mu(L_5)$ above the highest critical value. By the Moser regularisation, the Hamiltonian structure ω on $\Sigma_{\mu,c}$ extends to collisions and we get the Hamiltonian manifold $(\bar{\Sigma}_{\mu,c}, \bar{\omega})$. The Liouville 1-form $\lambda = p dq$, on the other hand, does not extend. We do, however, have a local primitive $\tilde{\lambda}$ of $\bar{\omega}$ in a neighbourhood U of collision at each primary because the fibre is Lagrangian and so ω vanishes on the intersection of the regularised hypersurface with the fibre over $p = \infty$. On the intersection $V := \Sigma_{\mu,c} \cap U$ both $\lambda|_V$ and $\tilde{\lambda}|_V$ are primitives of $\bar{\omega}|_V = \omega|_V$, so $d(\lambda|_V - \tilde{\lambda}|_V) = 0$. The subset $V \subset \bar{\Sigma}_{\mu,c}$ is diffeomorphic to $S^*(\mathbb{R}^n \setminus \{0\})$, which has trivial fundamental group for $n = 3$. So in this case the first de Rham cohomology of V is trivial and the closed 1-form $\lambda|_V - \tilde{\lambda}|_V$ has a primitive $f \in C^\infty(V)$. Let $g \in C^\infty(V)$ be a smooth cut-off function which is identically zero on $\Sigma_{\mu,c}$ and identically one in a small neighbourhood of $p = \infty$ in U . Define

$$\bar{\lambda} := \begin{cases} \lambda & \text{in } \Sigma_{\mu,c} \setminus V \\ \lambda - d(gf) & \text{in } V \\ \tilde{\lambda} & \text{in } U \setminus V \end{cases}$$

as a smooth extension of $\lambda|_{\Sigma_{\mu,c} \setminus V}$ onto $\bar{\Sigma}_{\mu,c}$. For $n = 2$, V does have a large fundamental group, but we can simply define $\bar{\lambda}$ as the restriction of the three-dimensional construction. The minimal distance to collision for all second species orbits with non-parallel velocity vectors at collision gives us enough space for our small neighbourhood U . In that way the local change of primitive does not change the action of the orbit.

Using this notation, we can now explicitly state the main theorem which will be divided into the planar case $n = 2$ and the spatial case $n = 3$:

Theorem 5.3:

In the planar case we have:

For every $c \in [-\sqrt{2}, 0)$ and $r_0 \in \mathbb{R}$ there exists a $\mu_0 > 0$ such that for every $\mu \in (0, \mu_0]$ the Hamiltonian manifold $(\bar{\Sigma}_{\mu,c}, \bar{\omega})$ of the planar circular restricted three-body problem with mass ratio μ does not admit an $\bar{\omega}$ -compatible contact form α such that $[\alpha - \bar{\lambda}] = [r\beta_0] \in H_{\text{dR}}^1(\bar{\Sigma}_{\mu,c})$ for any coefficient $r \geq r_0$.

For the spatial case:

For every $c \in [-\sqrt{2}, 0)$ there exists a $\mu_0 > 0$ such that for every $\mu \in (0, \mu_0]$ the Hamiltonian manifold $(\Sigma_{\mu,c}, \omega)$ of the circular restricted three-body problem with mass ratio μ does not admit an ω -compatible contact form α .

Proof: We begin with the planar case: Let $c_0 \in [-\sqrt{2}, 0)$ and $r_0 \in \mathbb{R}$ be arbitrary. Then lemma 5.1 from above gives us an ordinary non-degenerate generating orbit γ_0 with energy c and action $\mathcal{A}(\gamma_0) < r_0 - \varepsilon$ for any $\varepsilon > 0$. By theorem 3.6 there exists a $\mu_0 > 0$ such that for all $\mu \in (0, \mu_0]$ there an orbit orbit γ_μ in the restricted three-body problem with mass ratio μ that has energy c and action $\mathcal{A}(\gamma_\mu) \in (\mathcal{A}(\gamma_0) - \varepsilon, \mathcal{A}(\gamma_\mu) + \varepsilon)$, i. e. $\mathcal{A}(\gamma_\mu) < r_0$. We have furthermore seen in lemma 5.2 that the continued orbits from

lemma 5.1 in the restricted three-body problem all have $\int \gamma_\mu^* \beta_0 = -1$.

Assume by contradiction that we have an $\bar{\omega}$ -compatible contact form $\alpha \in \Omega^1(\bar{\Sigma}_{\mu,c})$ such that $[\alpha - \bar{\lambda}] = [r\beta_0] \in H_{\text{dR}}^1(\bar{\Sigma})$ for an $r \geq r_0$. Then we can write $\alpha = \bar{\lambda} + r\beta_0 + \text{d}f$ and integrate

$$\int_{S^1} \gamma_\mu^* \alpha = \int_{S^1} \gamma_\mu^* (\bar{\lambda} + r\beta_0 + \text{d}f) = \int_{S^1} \gamma_\mu^* \bar{\lambda} + r \int_{S^1} \gamma_\mu^* \beta_0 = \mathcal{A}(\gamma_\mu) - r \leq \mathcal{A}(\gamma_\mu) - r_0 < 0.$$

This contradicts the fact that the integral over a compatible contact form along a Hamiltonian solution needs to be positive.

In the spatial case all constructed orbits are contractible since already $\Sigma_{\mu,c}$ has trivial fundamental group. Therefore, we directly get the claimed statement. \square

This concludes the main part of this work and in the remaining chapters we will first look at some numerical computations on these orbits and then discuss what questions arise and what future research could be suggested on this topic.

6 Numerical results

After the analytical results from the previous chapter we want to add some numerical computations to visualise the continuations for actual mass ratios. There will be two sections which both focus on direct orbits from sequences of section 4.4.2. In the first section we will fix the number of rotation I of M_2 around M_1 at 1 and vary θ , i. e. we will look at the first orbit in these sequences. For the second section we will fix a θ and look at the first several orbits in this sequence.

The data for generating orbits was obtained by numerically solving the timing condition (28) for the semi-major axis a and then computing the energy H_0 and the action \mathcal{A} from equations (37) and (39). The remaining parameter q_0 represents the apoapsis distance from the origin, which is the initial position of the orbit. Continued orbits for small mass ratios were found by using the symmetry (15) and shooting perpendicularly from the q_1 -axis while searching for perpendicular intersections when returning. The programming for finding these orbits was done in python using standard libraries for solving ODEs and integration. The results are numerical evidence of how far the described generating orbits might be followed and do not represent numerical or computer assisted proofs.

6.1 First orbit in sequence with varying intersection angle

Table 1 shows the data for generating orbits for $I = 1$ and varying θ from 0 to π . We use degrees instead of radians to describe the angle θ which will be incremented in 10 degree steps. From (39) we know that the action of generating orbits in the sequences with fixed $\theta \in (0, \pi]$ tends to $-\infty$ as $I \rightarrow \infty$. However, not all sequences always have negative action, as one can see in the case where θ is at 10 degrees. In the boundary case $\theta = 0$ the action of orbits in the sequence does not tend to negative values and is instead always positive. Figure 10 shows every third of these generating orbits in fixed

coordinates Q and in rotating coordinates q . We note the special cases $\theta = \pi$ where the deflection angle is zero, i. e. the generating orbit is non-ordinary, and $\theta = \pi/2$ where the deflection angle is $-\pi$ and even the continued orbit might collide with M_2 .

Table 2 shows the initial positions of these orbits when continued to the astronomical mass ratios $\mu \approx 0.000953$ of the Sun-Jupiter system, $\mu \approx 0.012143$ of the Earth-Moon system and $\mu \approx 0.108511$ of the Pluto-Charon system. These mass ratios were chosen for the relevance in our solar system: The Sun-Jupiter system has the largest mass ratio of all the planets in relation to the sun and governs many phenomena like the occurrence of asteroids. Obviously, the Earth-Moon system is of major importance to us and plays a large part in near-Earth satellites and lunar space missions. Pluto and Charon have the largest mass ratio of a binary system in our solar system and serves as the largest mass ratio we will have to deal with in our current reach. Table 3 adds some larger non-astronomical values as well. In all the continuations the same energy value is held as the generating orbit in accordance with theorem 3.6.

We can see that smaller values of θ seem to continue up to higher mass ratios as opposed to larger values of θ . Here, after some point no orbit could be found nearby and the corresponding entries are marked with an “x”. This makes good sense since the limit orbits at $\theta = \pi$ are bifurcation orbits and here two intersecting families of generating orbits split in the continuation and move away from the original bifurcation orbit.

Also the action of continued orbits seems to always be slightly larger than that of the generating orbit. On the other hand, even the first generating orbits in most of these sequences yield negative action, especially for large values of θ . The smallest energy where one gets a generating orbit with negative action is already very close to the critical value $-3/2$. Although these are only isolated orbits, one might now expect that there is an obstruction for the restricted three-body problem to be of contact type for all energies between 0 and the highest critical value $H_\mu(L_5)$.

6.2 Sequence at 10 degrees intersection angle

We now take a closer look at the first sequence from 1 where the intersection angle θ is nonzero. This was the only one where the action of the first orbit is nonnegative. So, we are firstly interested in how quickly the action becomes negative, but also if we can still continue the generating orbit to the large mass ratio of $\mu = 0.5$ as the sequence goes on.

These generating orbits are computed in table 4 and we see that the action becomes negative at the 10th orbit in the sequence. Furthermore, we can see the energy slowly converging to $-\sqrt{1 - \cos(\pi/18)} \approx -0.123256$ while the semi-major axis grows. Tables 5 and 6 show again the continued orbits to the same mass ratios as before. Here, we notice that also the higher orbits in the sequence so far all continue all the way up to $\mu = 0.5$ and eventually even the action becomes negative for this large mass ratio. This evidence suggests that the restricted three-body problem might not be of contact type in between the highest critical value and zero for any mass ratio $\mu \in (0, 1)$. Note, as mentioned in section 4.4.2, that all orbits with even I belong to the same family f and all orbits with odd I belong to family h in Hénon’s notation. This is visualised in figure 11 where the generating and continued orbits of this sequence are depicted for the first three $I = 1, 2, 3$.

θ	a	q_0	H_0	\mathcal{A}
0	1.114891	2.229783	-0.448474	1.434641
10	1.151460	2.289513	-0.597508	0.472433
20	1.191803	2.331984	-0.737353	-0.479144
30	1.234738	2.358649	-0.865060	-1.392612
40	1.278895	2.371414	-0.978834	-2.246054
50	1.322831	2.372473	-1.077948	-3.024066
60	1.365152	2.364145	-1.162569	-3.717803
70	1.404646	2.348721	-1.233529	-4.324279
80	1.440377	2.328356	-1.292090	-4.845201
90	1.471746	2.304988	-1.339732	-5.285607
100	1.498494	2.280307	-1.377985	-5.652556
110	1.520668	2.255753	-1.408307	-5.954007
120	1.538560	2.232546	-1.432015	-6.197965
130	1.552639	2.211726	-1.450243	-6.391878
140	1.563480	2.194211	-1.463929	-6.542246
150	1.571719	2.180859	-1.473821	-6.654366
160	1.578013	2.172531	-1.480481	-6.732160
170	1.583022	2.170155	-1.484294	-6.777997
180	1.587401	2.174802	-1.485467	-6.792454

Table 1: Generating orbits for $I = 1$ and θ in degrees.

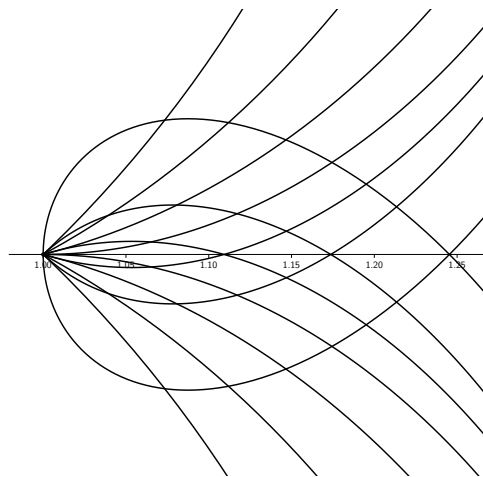
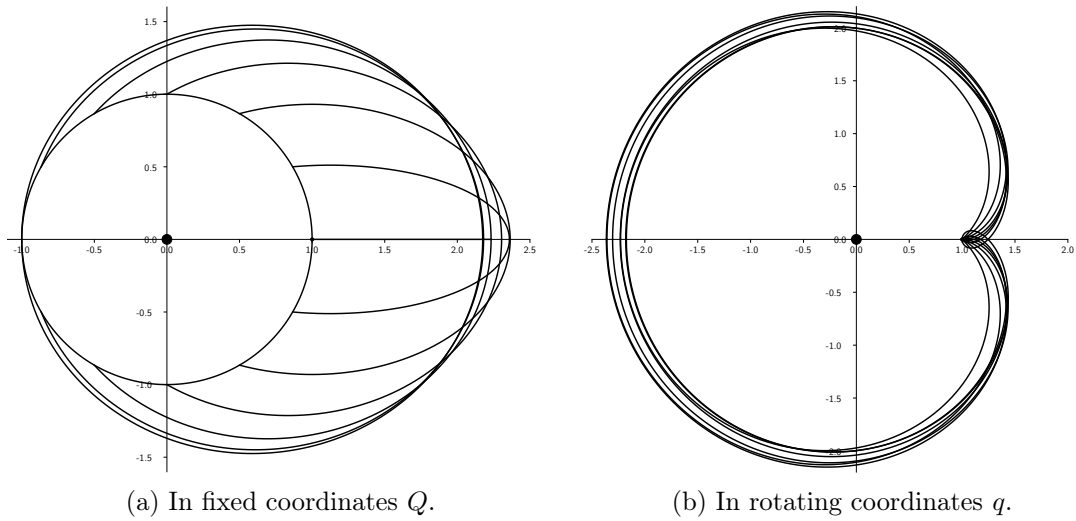


Figure 10: Generating orbits for $I = 1$ and varying θ from 0 to π in steps of 10 degrees.

θ	Sun-Jupiter		Earth-Moon		Pluto-Charon	
	q_0	\mathcal{A}	q_0	\mathcal{A}	q_0	\mathcal{A}
0	2.229061	1.446733	2.220504	1.546640	2.142401	2.136580
10	2.288901	0.485253	2.281639	0.590492	2.216384	1.209834
20	2.331460	-0.465552	2.325234	-0.355078	2.269946	0.288979
30	2.358198	-1.378186	2.352824	-1.262459	2.305515	-0.597382
40	2.371026	-2.230715	2.366375	-2.109609	2.325631	-1.426317
50	2.372143	-3.007720	2.368130	-2.881020	2.332950	-2.181565
60	2.363871	-3.700338	2.360452	-3.567767	2.330171	-2.853621
70	2.348508	-4.305571	2.345684	-4.166823	2.319969	-3.439064
80	2.328214	-4.825112	2.326039	-4.679890	2.305002	-3.939387
90	2.304939	-5.263994	2.303542	-5.112050	2.288258	-4.359638
100	2.280390	-5.629270	2.280016	-5.470452	2.281012	-4.707251
110	2.256040	-5.928906	2.257156	-5.763208	x	x
120	2.233168	-6.170932	2.236858	-5.998577	x	x
130	2.212958	-6.362855	x	x	x	x
140	2.196764	-6.511324	x	x	x	x
150	2.190318	-6.622143	x	x	x	x
160	x	x	x	x	x	x
170	x	x	x	x	x	x
180	x	x	x	x	x	x

Table 2: Continued orbits for $I = 1$ and θ in degrees for astronomical mass ratios.

θ	$\mu = 0.2$		$\mu = 0.5$	
	q_0	\mathcal{A}	q_0	\mathcal{A}
0	2.059605	2.593750	x	x
10	2.150085	1.693790	1.816536	3.069224
20	2.215887	0.792632	1.992154	2.275666
30	2.261108	-0.079578	2.113013	1.462972
40	2.289277	-0.898644	x	x
50	2.303809	-1.647264	x	x
60	2.308293	-2.315120	x	x
70	2.307463	-2.898274	x	x
80	x	x	x	x
90	x	x	x	x
100	x	x	x	x
110	x	x	x	x
120	x	x	x	x
130	x	x	x	x
140	x	x	x	x
150	x	x	x	x
160	x	x	x	x
170	x	x	x	x
180	x	x	x	x

Table 3: Continued orbits for $I = 1$ and θ in degrees for non-astronomical mass ratios.

I	a	q_0	H_0	\mathcal{A}
1	1.151461	2.289514	-0.597508	0.472433
2	1.703950	3.397169	-0.439704	0.971722
3	2.180544	4.351247	-0.369431	1.179810
4	2.610411	5.211440	-0.328406	1.217261
5	3.007662	6.006225	-0.301045	1.142278
6	3.380347	6.751789	-0.281280	0.986919
7	3.733587	7.458411	-0.266220	0.770813
8	4.070887	8.133123	-0.254297	0.506915
9	4.394782	8.781000	-0.244582	0.204272
10	4.707173	9.405855	-0.236486	-0.130527
11	5.009538	10.010645	-0.229617	-0.492519
12	5.303051	10.597720	-0.223702	-0.877859
13	5.588663	11.168989	-0.218546	-1.283506
14	5.867162	11.726026	-0.214003	-1.707004
15	6.139207	12.270150	-0.209966	-2.146341
16	6.405358	12.802481	-0.206349	-2.599845
17	6.666093	13.323979	-0.203088	-3.066108
18	6.921829	13.835474	-0.200128	-3.543935
19	7.172927	14.337693	-0.197428	-4.032299
20	7.419707	14.831273	-0.194953	-4.530312

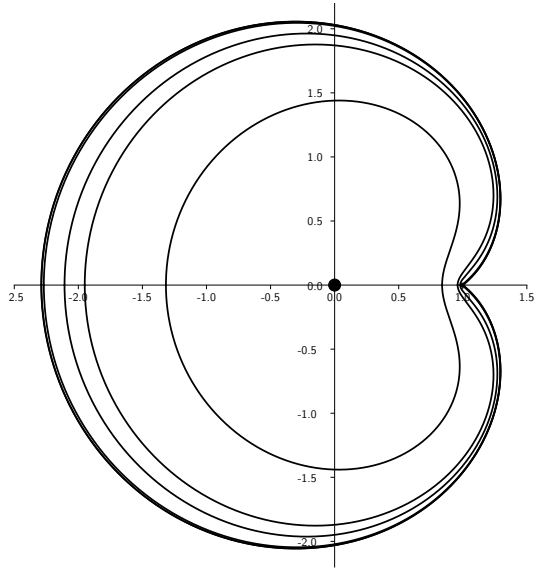
Table 4: Generating orbits for fixed $\theta = \pi/18$.

	Sun-Jupiter		Earth-Moon		Pluto-Charon	
I	q_0	\mathcal{A}	q_0	\mathcal{A}	q_0	\mathcal{A}
1	2.288901	0.485253	2.281639	0.590492	2.216384	1.209834
2	3.396803	0.984282	3.392470	1.089921	3.353351	1.733091
3	4.350951	1.192265	4.347446	1.297962	4.315925	1.949195
4	5.211184	1.229658	5.208155	1.335366	5.180883	1.990792
5	6.005993	1.154636	6.003252	1.260344	5.978585	1.918388
6	6.751575	0.999251	6.749047	1.104955	6.726282	1.764807
7	7.458211	0.783125	7.455838	0.888823	7.434486	1.550010
8	8.132933	0.519211	8.130687	0.624905	8.110475	1.287122
9	8.780818	0.216555	8.778675	0.322245	8.759385	0.985285
10	9.405681	-0.118255	9.403624	-0.012570	9.385118	0.651146
11	10.010477	-0.480255	10.008494	-0.374574	9.990653	0.289708
12	10.597558	-0.865603	10.595640	-0.759926	10.578382	-0.095163
13	11.168832	-1.271256	11.166970	-1.165583	11.150223	-0.500404
14	11.725873	-1.694760	11.724061	-1.589089	11.707773	-0.923547
15	12.270001	-2.134103	12.268235	-2.028434	12.252356	-1.362572
16	12.802335	-2.587611	12.800611	-2.481946	12.785104	-1.815798
17	13.323836	-3.053878	13.322149	-2.948216	13.306981	-2.281813
18	13.835334	-3.531709	13.833682	-3.426048	13.818826	-2.759415
19	14.337556	-4.020076	14.335935	-3.914418	14.321365	-3.247575
20	14.831139	-4.518092	14.829547	-4.412436	14.815244	-3.745402

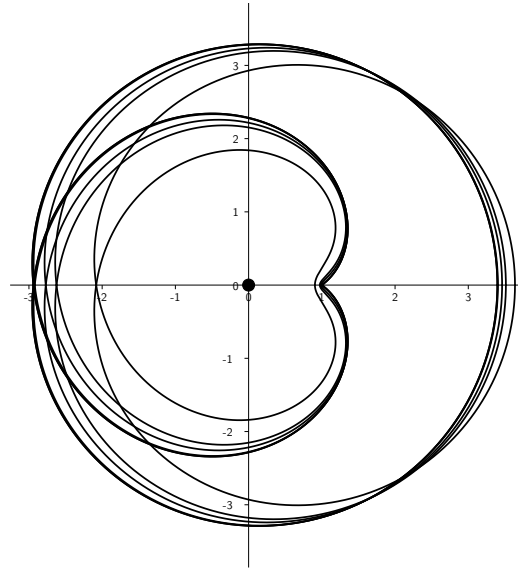
Table 5: Continued orbits for fixed $\theta = \pi/18$ for astronomical mass ratios.

I	$\mu = 0.2$		$\mu = 0.5$	
	q_0	\mathcal{A}	q_0	\mathcal{A}
1	2.150085	1.693790	1.816536	3.069224
2	3.313535	2.246562	3.137846	3.758241
3	4.283998	2.472591	4.146060	4.022613
4	5.153181	2.519383	5.033830	4.088841
5	5.953545	2.450237	5.846074	4.031746
6	6.703154	2.298919	6.603994	3.888747
7	7.412800	2.085796	7.319979	3.681770
8	8.089940	1.824206	8.002119	3.424935
9	8.739790	1.523409	8.656086	3.127945
10	9.366317	1.190125	9.286061	2.797789
11	9.972531	0.829403	9.895240	2.439691
12	10.560854	0.445144	10.486136	2.057670
13	11.133216	0.040432	11.060773	1.654893
14	11.691232	-0.382250	11.620811	1.233905
15	12.236233	-0.820866	12.167634	0.796784
16	12.769361	-1.273728	12.702410	0.345255
17	13.291585	-1.739416	13.226138	-0.119236
18	13.803747	-2.216723	13.739680	-0.595463
19	14.306580	-2.704616	14.243785	-1.082372
20	14.800730	-3.202198	14.739113	-1.579057

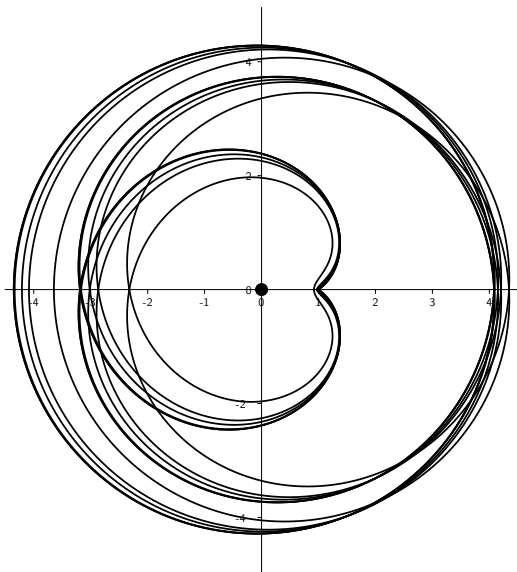
Table 6: Continued orbits for fixed $\theta = \pi/18$ for nonastronomical mass ratios.



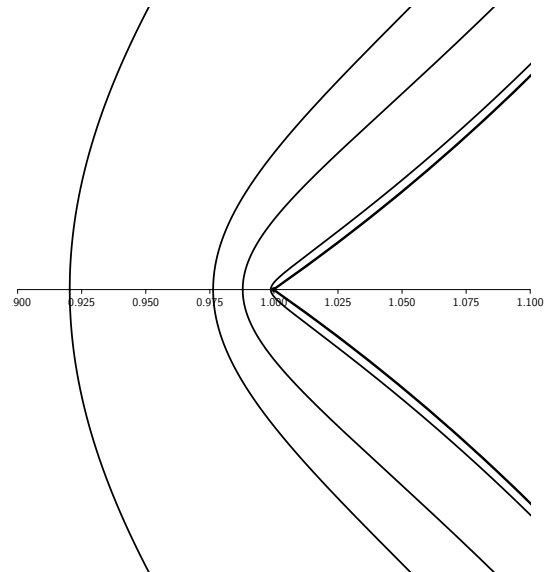
(a) $I = 1$



(b) $I = 2$



(c) $I = 3$



(d) Close-up view of the neighbourhood of M_2 .

Figure 11: Generating orbit and continued orbits for $\theta = \pi/18$.

References

- [AFvKP12] Peter Albers, Urs Frauenfelder, Otto van Koert, and Gabriel P. Paternain. Contact geometry of the restricted three-body problem. *Comm. Pure Appl. Math.*, 65(2):229–263, 2012.
- [Alb19] Alain Albouy. Lambert’s theorem: Geometry or dynamics? *Celest Mech Dyn Astr*, 131(40), 2019.
- [Are63] Richard F. Arenstorf. Periodic solutions of the restricted three body problem representing analytic continuations of keplerian elliptic motions. *American Journal of Mathematics*, 85:27, 1963.
- [AU20] Alain Albouy and Antonio J. Ureña. Some simple results about the lambert problem. *Eur. Phys. J. Spec. Top.*, 229, 2020.
- [Bir14] George D. Birkhoff. The restricted problem of three bodies. *Rendiconti del Circolo Matematico di Palermo*, 39:265–334, 1914.
- [BM00] Sergey V. Bolotin and Robert S. Mackay. Periodic and chaotic trajectories of the second species for the n -centre problem. *Celestial Mech. Dynam. Astronom.*, 77(1):49–75 (2001), 2000.
- [Bru94] Alexander D. Bruno. *The Restricted 3-Body Problem: Plane Periodic Orbits*. De Gruyter, Berlin, New York, 1994.
- [Cel06] Alessandra Celletti. Basics of regularization theory. In *Chaotic Worlds: From Order to Disorder in Gravitational N-Body Dynamical Systems*, pages 203–230, Dordrecht, 2006. Springer Netherlands.
- [CJK20] Wanki Cho, Hyojin Jung, and Geonwoo Kim. The contact geometry of the spatial circular restricted 3-body problem. *Abhandlungen aus dem Mathematischen Seminar der Universität Hamburg*, 90(2):161 – 181, 2020.
- [Hag70] Yusuke Hagihara. *Dynamical principles and transformation theory*, volume 1 of *Celestial Mechanics*. MIT Press, 1970.
- [Hén97] Michel Hénon. *Generating families in the restricted three-body problem*, volume 52 of *Lecture Notes in Physics. New Series m: Monographs*. Springer-Verlag, Berlin, 1997.
- [Lam61] Johann H. Lambert. *Insigniores orbitae cometarum proprietates*. Eberhard Klett, Augusta Vindelicorum (Augsburg), 1761.
- [Poi92] Henri Poincaré. *Les méthodes nouvelles de la mécanique céleste*, volume 1. Gauthier-Villars, Paris, 1892.
- [Poi99] Henri Poincaré. *Les méthodes nouvelles de la mécanique céleste*, volume 3. Gauthier-Villars, Paris, 1899.